An *in vivo* screen for proteolytic switch domains that can mediate Notch activation by force

Frederick Baker[1], Jacob Harman[1], Trevor Jordan[1], Breana Walton[1], Amber Ajamu-Johnson[1], Rama Alashqar[1], Simran Bhikot[1], Gary Struhl[2,3] and Paul D. Langridge[1]*

1 Department of Biological Sciences, Augusta University, Augusta, GA 30912, USA

2 Department of Genetics and Development, Columbia University, New York, NY, USA 10027

3 Mortimer B. Zuckerman Mind Brain Behavior Institute, New York, NY, USA, 10027

*Senior, corresponding author, lead contact.

Abstract

Notch proteins are single pass transmembrane receptors activated by sequential extracellular and intramembrane cleavages that release their cytosolic domains to function as transcription factors in the nucleus. Upon binding, Delta/Serrate/LAG-2 (DSL) ligands activate Notch by exerting a "pulling" force across the intercellular ligand/receptor bridge. This pulling force is generated by Epsin-mediated endocytosis of ligand into the signal-sending cell, and results in the extracellular cleavage of the force-sensing Negative Regulatory Region (NRR) of the receptor by an ADAM10 protease [Kuzbanian (Kuz) in *Drosophila*]. Here, we have used chimeric Notch and DSL proteins to screen for other domains that can function as ligand-dependent proteolytic switches in place of the NRR in the developing *Drosophila* wing. While many of the tested domains are either refractory to cleavage or constitutively cleaved, we identify several that mediate Notch activation in response to ligand. These NRR analogues derive from widely divergent source proteins and have strikingly different predicted structures. Yet, almost all depend on force exerted by Epsin-mediated ligand endocytosis and cleavage catalyzed by Kuz. We posit that the sequence space of protein domains that can serve as force-sensing proteolytic switches in Notch activation is unexpectedly large, a conclusion that has implications for the mechanism of target recognition by Kuz/ADAM10 proteases and is consistent with a more general role for force dependent ADAM10 proteolysis in other cell contact-dependent signaling

mechanisms. Our results also validate the screen for increasing the repertoire of proteolytic switches available for synthetic Notch (synNotch) therapies and tissue engineering.

Introduction

Many processes in biology depend on contact-dependent, juxtacrine signaling in which transmembrane ligands and receptors form intercellular bridges between "sending" and "receiving" cells. Such bridges are likely exposed to pulling forces as one or both ends of the bridge undergo endocytosis and the resulting mechanical tension across the bridge can lead to ectodomain cleavages that regulate signaling. A prototypical example is the receptor Notch, a highly conserved single pass transmembrane protein that has profound and pervasive roles in development, physiology and disease (Greenwald 1998; Gazave et al. 2009; Kovall et al. 2017). Notch is activated by single pass transmembrane ligands of the conserved Delta/Serrate/LAG-2 (DSL) family. Upon binding, DSL ligands induce cleavage and shedding of the Notch ectodomain by an ADAM10 protease tethered to the surface of the receiving cell (Pan and Rubin 1997; Brou et al. 2000; Lieber, Kidd, and Young 2002). Ectodomain shedding renders the rest of the receptor a substrate for intramembrane cleavage by γ-secretase (De Strooper et al. 1999; Struhl and Greenwald 1999; Struhl and Adachi 2000), releasing the cytosolic domain—a transcription factor—for entry into the nucleus (Kidd, Lieber, and Young 1998; Lecourtois and Schweisguth 1998; Schroeter, Kisslinger, and Kopan 1998; Struhl and Adachi 1998).

For Notch, activation depends on mechanical tension exerted across the intercellular ligand/receptor bridge by endocytosis of the ligand into the sending cell. Specifically, upon binding to Notch, DSL ligands are recruited to the Clathrin endocytic pathway by the adapter protein Epsin (Overstreet, Fitch, and Fischer 2004; Wang and Struhl 2004; Wang and Struhl 2005). The process of ligand recruitment and/or internalization then generates a pulling force across the ligand/receptor bridge that renders it subject to

ADAM10 proteolysis (Gordon et al. 2015; Langridge and Struhl 2017). Both *in vivo* and biophysical studies indicate that cleavage depends on the exposure of an otherwise buried site in a conserved, juxtamembrane "Negative Regulatory Region" (NRR) that behaves as a force sensitive proteolytic switch (Gordon et al. 2015; Sloas et al. 2023). Indeed, the key role of the NRR can be recapitulated using a well-defined, force-dependent proteolytic switch—the A2 domain of Von Willebrand Factor (Tsai, Sussman, and Nagel 1994; Zhang et al. 2009) - in place of the NRR, provided it is tuned to the appropriate force level (Langridge and Struhl 2017).

The ectodomains of many other cell surface proteins are also cleaved by ADAM10 proteases (Hayashida et al. 2010; Tosetti et al. 2021), raising the possibility that force-dependent, ADAM10 proteolysis plays a more general role in juxtacrine signaling mechanisms. In support, although many ADAM10 substrate proteins are cleaved constitutively [e.g. (Weskamp et al. 2006)], proteolysis of at least some depends on ligand (Pan and Rubin 1997; Janes et al. 2005). However, the sheer number of ADAM10 substrates identified to date [at least 100 (Lichtenthaler, Lemberg, and Fluhrer 2018)], as well as the lack of a defined consensus cleavage site (Caescu, Jeschke, and Turk 2009), make it difficult to assess the prevalence of ADAM10-dependent force-sensitive switches in juxtacrine signaling. Moreover, the possibility that any given ADAM10-sensitive domain functions as a proteolytic switch needs to be validated by experiment. Notably, such tests have been performed in a cell culture screen of Sea urchin Enterokinase Agrin-like (SEA) domains, which have structural similarity with Notch NRRs and are found in many transmembrane receptors and other cell surface proteins (Hayward, Aird, and Gordon 2019). The capacity of SEA domains to function as NRR-like proteolytic switches in cell culture is consistent with a more general role for such domains in force-sensitive signaling events. However, it is unclear how well cell culture conditions capture the native signaling processes *in vivo*, where the relevant interactions often occur between cells in polarized epithelia, and for which ligand and/or receptor endocytosis may be necessary to generate the requisite, activating force.

Here we present the results of an *in vivo* screen designed to identify protein domains that can function as proteolytic switches in place of the Notch NRR. The screen is predicated on the use of chimeric forms of *Drosophila* Notch and Delta in which the native ligand and receptor ectodomains are replaced by heterologous ligand and receptor binding domains, and productive signaling monitored *in vivo* by the induction of Notch target genes in wing imaginal discs (Langridge and Struhl 2017). Of 43 chimeric Notch receptors that contain different candidate switch domains in place of the native Notch NRR, we have identified 11 that respond to ligand in an Epsin and Kuz dependent manner. Strikingly, these proteolytic switches derive from a wide range of protein domains and appear remarkably diverse in structure, indicating that the repertoire of possible switch domains is surprisingly large and suggesting that many different cell surface proteins have the potential to be force-dependent targets for Kuz/ADAM10 proteases. Our results also validate the screen as a means to identify new switch domains that can be used to diversify the collection of available synthetic Notch (synNotch) receptors for biomedical applications (Morsut et al. 2016; Roybal et al. 2016).

Results

In vivo screen for putative force sensitive proteolytic switches able to substitute for the Notch Negative Regulatory Region (NRR)

To screen protein sequences for their capacity to function as NRR-like proteolytic switches, we generated transgenes that encode chimeric Notch receptors in which (i) the ligand-binding, EGF-repeat domain of the native receptor is replaced by the ligand-binding domain of the Follicle Stimulating Hormone Receptor (FSHR), and (ii) the juxtamembrane NRR is replaced by candidate force sensors from other proteins (Fig. 1A). All such FSHR-Notch receptors retain the transmembrane and downstream intracellular domains of the native Notch receptor. Hence, when activated, they drive well-characterized transcriptional and morphological outputs of the Notch signaling

pathway. We then asked whether each of these receptors can be activated *in vivo* by a chimeric form of Delta (Dl) in which the native ectodomain is replaced by Follicle Stimulating Hormone (FSH-Dl). Importantly, native FSH is a heterodimer of distinct α and β subunits. As in our prior studies (Langridge and Struhl 2017; Langridge et al. 2022), we generate the functional FSH-Dl ligand by co-expressing an otherwise inactive FSHβ-Dl ligand together with secreted FSHα. Because virtually all of our experiments are performed in the presence of co-expressed FSHα, we refer to the FSHβ-Dl coding sequence and encoded protein—for convenience—as FSH-Dl, except when we perform negative controls in which it is expressed in the absence of FSHα.

To execute this approach at scale, we incorporated three strategies to optimize generating chimeric FSHR-Notch receptors and testing their capacity to respond to FSH-Dl.

First, the coding sequences for a collection of FSHR-Notch chimeric receptors, each having a different protein domain in place of the native NRR, were introduced into a series of transformation vectors bar-coded by using different transgenic markers (e.g., variously deleted forms of a genomic *yellow*$^{+}$ rescuing fragment that generate different patterns of body and bristle pigmentation). This allowed us to micro-inject mixtures of several transgenes at a time, and then distinguish transformants of each transgene by phenotype, thus saving time, materials and cost (Fig. 1B).

Second, we used transformation vectors designed to be compatible with our Mosaic Analysis by Promoter Swap (MAPS) technique (Langridge and Struhl 2017). This allows us to generate potential signaling interfaces between clones of FSH-Dl expressing cells and surrounding FSHR-Notch expressing tissue. Specifically, the coding sequences of the chimeric FSHR-Notch receptors were placed downstream of an *Upstream Activating Sequence* (*UAS*) promoter controlled by the yeast Gal4 transcription factor (Brand and Perrimon 1993), but separated from the promoter by a target for mitotic

recombination catalyzed by the yeast Flp recombinase [FRT, symbolized by ">" (Golic 1991)]. All of the resulting *UAS>FSHR-Notch* transgenes were inserted at the same attP genomic docking site [at cytological position 86Fb (Bischof et al. 2007)] and in the same orientation as a *Ø>FSH-Dl* transgene that lacks a functional promoter ("*Ø*") (Langridge and Struhl 2017). Consequently, transheterozygous *UAS>FSHR-Notch/Ø>FSH-Dl* cells express only FSHR-Notch in response to Gal4. However, when subjected to heat shock induced Flp recombinase, these cells can undergo mitotic recombination across the FRTs to generate single cells in which the *UAS* promoter now drives expression of the ligand rather than the receptor [Fig. 1C; described in detail (Langridge and Struhl 2017)]. During subsequent development, these *UAS>FSH-Dl* founder cells form clones in a surround of *UAS>FSHR-Notch* tissue.

Third, we used a *nubbin.Gal4* (*nub.Gal4*) transgene to drive expression of the *UAS* transgenes in the "pouch" of the wing imaginal disc—a circular domain within the disc destined to form the adult wing. Normally, peak DSL/Notch signaling in the pouch is restricted to a thin stripe of cells flanking the dorso-ventral (D/V) boundary, where it (i) induces expression of the transcription factor Cut, (ii) specifies formation of wing margin bristles, and (iii) directs local production of Wingless (Wg), a morphogen that controls wing growth (Diaz-Benjumea and Cohen 1995; de Celis, Garcia-Bellido, and Bray 1996; Doherty et al. 1996). Accordingly, early heat shock induction of *UAS>FSH-Dl* clones in *UAS>FSHR-Notch/Ø>FSH-Dl* wing discs with *nub.Gal4* generates clonal interfaces between dedicated FSH-Dl and FSHR-Notch expressing cells. If a given FSHR-Notch chimera can be activated by FSH-Dl, these interfaces will induce ectopic Notch activation, the formation of ectopic wing margin bristles and altered wing morphology (Fig. 1D). Because activity of *nub.Gal4* is limited predominantly to the prospective wing, flies in which such ectopic signaling occurs are viable, fertile and otherwise phenotypically wild type.

To perform the screen (Fig. 1D), G_0 flies derived from embryos micro-injected with

each mixture of *UAS>FSHR-Notch* transgenes were outcrossed to screen their G_1 progeny for transgene insertions identified by the marker barcode. Females carrying each transgene were then outcrossed to "tester" males carrying the *nub.Gal4*, *Ø>FSH-Dl*, *UAS.FSHα* and *hsp70.flp* transgenes, heat-shocked early in larval life to generate clones, and the resulting *UAS>FSHR-Notch/Ø>FSH-Dl* adults scored for abnormal wing phenotypes indicating ectopic FSHR-Notch activation by the FSH-Dl ligand (Fig. 1D)

UAS>FSHR-Notch transgenes that score positively in the wing assay encode FSHR-Notch receptors that are either ligand-dependent or constitutively active. These two possibilities were distinguished in the test cross of *UAS>FSHR-Notch* females to *UAS.FSHα; Ø>FSH-Dl* males as only female progeny co-express FSHα, which is required for ligand activity (Fig. 1D, top), whereas male progeny do not. Accordingly, *UAS>FSHR-Notch* transgenes that cause abnormal wings in male progeny encode constitutively active receptors, the severity of the abnormalities providing an indication of the strength of the activity (Fig. 1D, bottom).

Conversely *UAS>FSHR-Notch* transgenes that score negatively encode receptors that are refractory to activation by ligand, consistent with the candidate domain not deriving from a proteolytic switch. However, a bona fide force sensor might nevertheless score negatively for a number of reasons. These include: (i) it's tuned to a sufficiently high force threshold such that it cannot be activated by FSH-Dl [*e.g.*, as is the case for the native A2 domain from VWF (Langridge and Struhl 2017)], (ii) it's cleaved sufficiently far amino-terminal from the receptor transmembrane domain to obviate cleavage by γ-secretase (Struhl and Adachi 2000), (iii) the candidate domain being tested is inadvertently truncated and hence an inoperable form of the native switch domain, or (iv) it is impaired by adventitious interactions with neighboring protein sequences. Hence, we draw no conclusions about the chimeric receptors that test negatively, but instead, have focused our analysis exclusively on *UAS>FSHR-Notch* transgenes that yielded positive results.

We present, below, the results of a screen of 43 *UAS>FSHR-Notch* transgenes, each encoding a different candidate proteolytic switch domain.

Protein domains tested for NRR-like proteolytic switch properties

We chose to test domains from a broad class of proteins to assess the efficacy of the screen as well as the range of structures that can mediate Notch cleavage in response to force (Table 1). Kuzbanian/ADAM10 proteolysis typically targets the juxtamembrane extracellular regions of surface proteins, and the amino acid sequence cleaved varies among substrates. Hence, we mostly tested domains positioned immediately N-terminal to the transmembrane domain of cell surface proteins involved in juxtacrine signaling and did not restrict the choice to domains with particular structural features. We also included a small number of miscellaneous peptide sequences and protein domains. Candidate domains differed in length and structural composition, ranging from juxtamembrane regions from surface receptors (e.g. from Dscam) to proteolytic switches previously identified in cell culture [SEA domains (Hayward, Aird, and Gordon 2019)], to unstructured domains (e.g., flagelliform, a spider silk protein that is a concatemer of glycine-proline-alanine repeats), to protein domains suggested by prior serendipitous findings (e.g., Venus fluorescent protein), to a few truncated versions of the native Notch NRR. Finally, for benchmarks, we used the intact NRRs of *Drosophila* Notch and the *C.elegans* Notch homologue LIN-12, which we have characterized in previous work (Langridge and Struhl 2017; Langridge et al. 2022).

Classification of candidate proteolytic switches based on Notch target gene expression

To corroborate and extend our initial classification of FSHR-Notch receptors that scored positively based on the initial wing assay, we repeated the MAPS experiments, this time analyzing the expression of the Notch target gene, *cut*, as monitored by staining for Cut protein, in the developing wing imaginal disc. Cut expression in the wing primordium is normally restricted to a thin strip of cells along the dorso-ventral (D/V) compartment

boundary in response to peak Notch activation (Fig. 2A). Hence, both ligand-dependent and constitutively active FSHR-Notch receptors should cause ectopic Cut expression, whereas receptors that are refractory to activation should not. By design, the canonical FSH-Dl and FSHR-Notch proteins are epitope tagged, respectively, with Horse Radish Peroxidase (HRP) and Cherry fluorescent protein (Fig. 1A). As a consequence, both *UAS>FSH-Dl* clones and the surrounding *UAS>FSHR-Notch* tissue can be identified with single cell resolution by monitoring HRP and/or Cherry expression, allowing inductive signaling and constitutive activity to be assayed by monitoring for ectopic Cut expression at or away from the clone borders.

The 43 transgenes fell into one of three categories that could be clearly distinguished in the wing imaginal disc: *UAS>FSHR-Notch* transgenes that had (i) no ectopic Cut expression scored as refractory to cleavage, (ii) Cut expression in FSHR-Notch expressing cells not close to FSH-Dl scored as constitutive, and (iii) ectopic Cut expression largely restricted to FSHR-Notch expressing cells that abut FSH-Dl expressing cells scored as ligand-dependent (Fig. 2B).

Of the 43 FSHR-Notch chimeric receptors assayed in this study, 20 scored negatively, as indicated by the failure to detect any departure from normal wing morphology in the MAPS outcross assay or through examination of Cut expression in the wing imaginal disc, whereas the remaining 23 scored positively (Table 1). Of these 23, 12 behaved as constitutively active, consistent with many ADAM10 substrates being subject to constitutive cleavage (Lichtenthaler, Lemberg, and Fluhrer 2018). However, the remaining 11 receptors fit the criteria for being ligand-dependent.

<u>Reliance of ligand-dependent FSHR-Notch receptors on Epsin-mediated ligand endocytosis</u>

Given our prior evidence that cleavage of the native NRR depends on the force generated by Epsin-mediated ligand endocytosis (Langridge and Struhl 2017), we next asked if the 11 ligand-dependent FSHR-Notch receptors are dependent on Epsin.

DSL/Notch signaling normally depends on ubiquitination of cytosolic lysine residues for recruitment to the Clathrin-endocytic pathway by Epsin (Wang and Struhl 2004; Wang and Struhl 2005). Hence, FSH-Dl ligands in which all lysines in the cytosolic domain are replaced by arginine (FSH-Dl-KtoR), or that lack a cytosolic domain entirely (FSH-Dl-ΔIC), are unable to enter the Clathrin pathway or to activate the canonical FSHR-Notch receptor (Langridge and Struhl 2017). Hence, to test whether activation of the 11 ligand-dependent receptors requires an Epsin endocytic "pull", we compared their responses to the wild type, KtoR, and ΔIC forms of FSH-Dl.

To perform this comparison, we have taken advantage of our previous findings that the distance from the D/V boundary that FSH-Dl/FSHR-Notch signaling can induce ectopic Cut expression provides an indication of the strength of signaling (Langridge and Struhl 2017). To normalize for variations in wing disc size, this measurement is expressed as the ratio of the maximum distance of ectopic Cut expression from the D/V boundary relative to the width of the D/V border. Previously, we have used this to provide evidence that the benchmark *Drosophila* Notch and LIN-12 NRRs are tuned to different force thresholds [Fig. 3A, (Langridge and Struhl 2017; Langridge et al. 2022)]. Using this approach, we found that the 11 candidate proteolytic switch domains fell into three distinct classes of force sensitivity.

The first class (5/11) behaved similarly to the native Notch NRR and contained protein domains from the receptors Deleted in Colorectal Cancer (DCC), Ephrin-type receptor B2 (EphB2) and *Drosophila* Eph (DEph), the *Drosophila* DSL ligand Serrate (Ser), and the human protocadherin FAT1. Specifically, they show a readily detectable response to FSH-Dl, but little or no response to FSH-Dl-KtoR or FSH-Dl-ΔIC, indicating a strong, if not absolute requirement for Epsin-dependent ligand endocytosis (Fig. 3B). This is similar to what we have observed previously for both the native Notch NRR as well as disease-associated mutant forms of the A2 domain from Von Willebrand Factor (Langridge and Struhl 2017), consistent with these 5 domains being tuned to respond to force thresholds similar to that of the native Notch NRR.

The second class (3/11) differs from the first in that the domains show a detectable response to FSH-Dl-KtoR and FSH-Dl-ΔIC, but one that is significantly weaker than their response to FSH-Dl (Fig. 3C). These domains came from Venus fluorescent protein (Venus), Down Syndrome Cell Adhesion Molecule (DSCAM) and Dystroglycan. Hence, they appear to be force-sensitive, but tuned to a sufficiently low force threshold that tonic mechanical tension across the intercellular ligand/receptor bridge may suffice to induce an activating cleavage. In this regard, they appear intermediate in their force tuning between the native *Drosophila* Notch NRR, which is strictly Epsin-dependent, and the *C. elegans* Notch NRR LIN-12, which is not [Fig. 3A, (Langridge et al. 2022)].

The third class (3/11) appears to be activated in a manner intermediate between ligand-dependent and constitutive receptors. These came from Flagelliform, EphrinB and a mutation of the fly Notch NRR (ΔLNR) that removes a portion of the heterodimerization domain and the three conserved Lin-12 Notch Repeats (LNR) that normally occlude the native Kuz cleavage site unless unfurled by force (Fig. 4). In these cases, we find that Cut is present at peak levels in FSHR-Notch expressing cells near FSH-Dl or FSH-Dl KtoR expressing cells but at much lower levels further away. In the absence of ligand, ectopic Cut expression can be detected, but it is restricted to the D/V boundary, where we infer it boosts the native response above the threshold sufficient to achieve detectable Cut expression. Hence, we interpret these receptors as being 'hypersensitive', having low constitutive activity as well as a readily detectable response to ligand, and this forms a sub-category of the ligand-dependent receptors (Table 1, chartreus).

We note that FSHR-Notch receptors carrying the different ligand-dependent domains show a wide range of responses to FSH-Dl, as monitored by the distance over which Cut can be induced away from the D/V boundary (Fig. 3). However, given (i) that transmembrane domain cleavage by γ-secretase depends on the size of the residual ectodomain stub left behind after ectodomain shedding (Struhl and Adachi 2000), and (ii) that we don't know where the different candidate domains are cleaved, we do not

draw any inferences about differences in force tuning based on the spatial responses of the different FSHR-Notch receptors to FSH-Dl. Instead, we draw such inferences only from comparing the responses of the same FSHR-Notch receptor to FSH-Dl versus FSH-Dl-KtoR or FSH-Dl-ΔIC, which we interpret as indicating the relative reliance on Epsin-dependent endocytic force.

Candidate force sensitive domains require the ADAM protease Kuzbanian for cleavage

The 11 force sensitive candidate domains, as well as the 12 domains that are constitutively cleaved, have little common sequence similarity and remarkable structural diversity based on AlphaFold predictions (Fig. S1). This could be because there are few, if any, domain-intrinsic sequence and structural prerequisites for cleavage by ADAM10/Kuz, or because the candidate switch domains are cleaved by other proteases. Hence, we tested the requirement for Kuz for the cleavage of these domains. To do this we employed permutations of MAPS technology, one for the ligand-dependent receptors and another for the constitutively active receptors (detailed in Figs. 5A and 6A,B). For both, we depended on the following RNA knock-down approach to greatly reduce Kuz activity in FSHR-Notch expressing cells.

Briefly, expression of *UAS.Kuz-RNAi* under *nub.Gal4* control in otherwise wildtype wing discs renders Cut undetectable at the DV boundary, indicating strongly reduced Kuz activity. However, this knock-down can be rescued cell-autonomously by co-expression of a *UAS.KuzHA* transgene, which is expressed at a sufficiently high level to escape knock-down by the *Kuz-RNAi* (Coleman et al. 2010). Hence, in animals that are otherwise wildtype for the native *kuz* gene, *UAS.KuzHA/UAS.Kuz-RNAi* transheterozygous cells are wildtype for Kuz function and express HA tagged Kuz, whereas homozygous *UAS.Kuz-RNAi/UAS.Kuz-RNAi* cells do not express HA tagged Kuz and have greatly diminished Kuz function. Thus, by generating transheterozygotes in which *UAS.Kuz-RNAi* is distal to *UAS>FSHR-Notch* on one chromosome and *UAS.KuzHA* is distal to *Ø>FSH-Dl* on the other, we were able to use MAPS technology to compare the ability of FSH-Dl expressing cells to induce Cut expression in abutting FSHR-Notch

expressing cells depending on whether they retain or lacked Kuz activity (Fig. 5; described in detail in Fig. S2).

We applied this assay to the 8 strictly ligand-dependent FSHR-Notch receptors as well as the benchmark receptors containing the NRRs from *Drosophila* Notch and *C. elegans* LIN-12 (Fig. 5B). For all of these receptors, we found that FSH-Dl signal-sending cells could induce Cut in abutting FSHR-Notch signal-receiving cells but only if they retained Kuz function and were not subject to *Kuz-RNAi* knockdown (Fig. 5B).

We also examined the Kuz requirement for activation for all three hypersensitive receptors and a selection of 6 constitutively cleaved receptors. In these cases, the position of the receptor clone relative to the ligand clone is not crucial since each receptor shows activity in the absence of ligand. We therefore compared activation of the receptors in the presence or absence of the *UAS.Kuz-RNAi* transgene, using a "twin-spot" MAPS strategy to compare benchmark ligand-dependent and hyper-sensitive receptors (Fig. 6A) and a simpler, non-MAPS strategy to assess the constitutively active receptors (Fig. 6C). As shown in Figures 6B and 6D, the benchmark receptors carrying the Notch NRR and A2 E1638K domains are strictly Kuz dependent in this context, as are 4/6 of the constitutively active receptors. However, the remaining 2/6 constitutively active receptors appear to be cleaved in a Kuz-independent manner.

Hence, except for two possible exceptions, activation of all of the chimeric FSHR-Notch receptors tested, whether ligand-dependent, hypersensitive or constitutive, depends on cleavage by the Kuz protease.

Discussion/Conclusions

We present a readily scalable, *Drosophila* screen to identify protein domains that can substitute for the Negative Regulatory Region (NRR) of Notch and activate the receptor in response to Epsin-mediated ligand endocytosis. In an initial, proof-of-principle test of 43 candidate domains, around one quarter (11/43) have this capacity

and comprise a surprisingly diverse repertoire of seemingly unrelated structural motifs. Further, in every case, activation requires Kuzbanian (Kuz), the sole *Drosophila* ADAM10 protease responsible for cleaving the NRR to activate the native receptor. These results (i) validate the screen, (ii) provide insight into the structural basis and cleavage of force-sensitive proteolytic switches by ADAM10 proteases, and (iii) raise the possibility that force-sensitive signaling mechanisms may be more prevalent than currently appreciated.

A scalable screen to identify protein domains that are cleaved in response to force

In our initial screen of 43 candidate proteolytic switches, we were able to quickly and unequivocally identify around half (23/43) as capable of mediating Notch activation when introduced in place of the native, force-dependent NRR domain. Of these, 12/23 conferred constitutive activation, while the remaining 11/23 exhibited ligand-dependence, whether stringent (8/11) or more relaxed (3/11). Importantly, the initial designations made on the basis of alterations in adult wing morphology following simple genetic crosses were validated by subsequent investigations of target gene expression in developing wing imaginal discs. Further, we successfully utilized additional genetic paradigms to quickly and unequivocally determine the requirements for Epsin-dependent ligand endocytosis and Kuz proteolysis for each of the 11 "positive" proteolytic switches. Finally, we optimized the methods used to introduce transgenes encoding different chimeric receptors, providing the potential to scale up the screen to assess hundreds rather than tens of different candidate proteolytic switches.

As noted in the Results, there are several technical limitations in the screen. These include (i) a requirement for the candidate switches to be tuned to respond to the force level exerted by Epsin-dependent ligand endocytosis, (ii) the position of the cleavage site within the switch domain [which governs the efficacy of the subsequent γ-secretase cleavage of the transmembrane domain of the receptor required for signal transduction; (Struhl and Adachi 2000)], and (iii) the structural integrity of the candidate domain when inserted in place of the native Notch NRR. In addition, some of

the candidate switch domains were chosen based on their potential to function as proteolytic switches in their normal molecular contexts, and hence the domains do not represent a random sample. Nevertheless, we find it striking that around a quarter of the candidate domains behave as force-sensitive proteolytic switches. In our view, these results, as well as both the ease and efficiency of the methods employed, validate the screen as a means to explore the structural requirements and basic mechanisms of force-sensitive signaling mechanisms.

An unexpectedly large and diverse collection of sequences can behave as force-sensitive proteolytic switches

Our initial choice of candidate proteolytic switches was biased, in part, by prior evidence that other juxtacrine signaling systems aside from DSL/Notch might likewise depend on force-dependent cleavage mechanisms. These include Eph/Ephrin, Frazzled/DCC and the DSCAM family of proteins, all of which have roles in neuronal guidance (Zang, Chaudhari, and Bashaw 2021). Some of these proteins share phenomenology with the Notch receptor, including γ-secretase cleavage following ADAM10 cleavage (Janes et al. 2005), transendocytosis of parts of the ligand/receptor bridge from one cell to another (Marston, Dickinson, and Nobes 2003; Greene et al. 2014), and intracellular domains that may act as transcription factors (Coleman et al. 2010; Neuhaus-Follini and Bashaw 2015). Other protein domains we tested were chosen based on their structural or functional properties [(SEA domains (Hayward, Aird, and Gordon 2019); Flagelliform)], or serendipitous observations (e.g., Venus fluorescent protein). However, regardless of the justifications for choosing the candidates, the domains that tested positively for ligand, Epsin and Kuz dependent activation exhibit remarkable structural diversity as assessed by AlphaFold predictions. That we observe such diversity amongst candidates suggests that the rules governing the vulnerability of putative substrate domains to ADAM10 cleavage are surprisingly lenient and that the sequence space for force-dependent proteolytic switches is unexpectedly large. This could suggest that factors other than solely exposure of the

substrate cleavage site are important in the precise regulation of cleavage in different contexts. Possibilities include the action of tetraspanin proteins that place the protease active site at the substrate in a position poised for cleavage (Lipper et al. 2022) and autoinhibitory structures within the protease that potentially have a capacity to respond to mechanical tension (Seegar et al. 2017). Curiously, the ADAM10 protease that cleaves the A2 domain docks with native Von Willibrand factor, poised just above the occluded cleavage site to execute the cleavage if the site is rendered accessible by torsional strain (Crawley et al. 2011). Hence, at least some of the specificity for Kuz/ADAM10 cleavage of the Notch NRR may similarly depend on the docking of the protease to the receptor, whether directly or through a bridging protein. Since the proteolytic switches we have identified all operate in the context of the FSH-Dl/FSHR-Notch signaling paradigm in which the receptor retains only the transmembrane and intracellular domains of native Notch, any such docking of Kuz would presumably have to be to these domains.

Two other aspects of our findings are worthy of note. First, the 11 candidate domains that tested positively for ligand, Epsin and Kuz dependence appear to fall on a spectrum reflecting requirements for different levels of Epsin-mediated, endocytic force. Specifically, 5/11 are strictly dependent on Epsin-mediated ligand endocytosis, as determined by the failure to activate the receptor of modified forms of the chimeric ligand that cannot enter the Epsin pathway. In contrast, 3/6 of the remaining domains are weakly activated by such ligands indicating these receptors respond to tonic mechanical tension across the ligand/receptor bridge. The final 3/6 domains are classed hypersensitive since they respond to ligand that cannot enter the Epsin pathway, but also have modest constitutive activity, indicating they are subject to cleavage even in the absence of ligand. We infer that each of these three classes are tuned to respond to distinct levels of ligand-dependent force.

Interestingly, the hypersensitive class includes a partially deleted form of the Notch NRR that retains little else except the defined Kuz cleavage site, suggesting that the

peptide sequence containing the cleavage site retains some residual capacity to function as a force-sensitive proteolytic switch. Significantly, the properties of all of these candidate force sensors contrast with properties of the native NRR from the *C. elegans* Notch protein LIN-12 (Langridge et al. 2022). In this case, the receptor can be strongly activated by ligand, whether or not it has access to the Epsin pathway, but appears devoid of activity in the absence of ligand. We suggest that the LIN-12 NRR comprises a special class of proteolytic switch that has been evolutionarily selected to respond non-linearly, such that it can be activated even in the absence of Epsin-dependent endocytic force while remaining strongly ligand-dependent.

Second, a motivation for screening for new NRR-like proteolytic switches is the conjecture that force-dependent Kuz cleavage may apply to many different juxtacrine signaling interactions in addition to DSL/Notch signaling. The success of this initial screen in identifying a diverse repertoire of such switches is consistent with this possibility. Indeed, one clear implication is that it will be difficult, if not impossible, to anticipate the presence of such a switch in any given signaling protein by its sequence or structural properties. Instead, identification will depend on functional tests, ideally *in vivo*.

<u>Increasing the repertoire of proteolytic switches for synthetic Notch biomedical applications.</u>

Synthetic Notch (synNotch) technologies employing chimeric ligand and receptors to generate new, heterologous signaling systems offer significant potential for disease therapies and tissue engineering (Morsut et al. 2016; Roybal et al. 2016). Hence, it will be desirable to have synNotch receptors with distinct characteristics that are optimized for certain contexts and applications, such as signaling within or between epithelia or in interactions with motile cells (e.g., lymphocytes). The cleavage domains identified in this study may well impart useful characteristics on synNotch activation, such as a distinct force tuning or signal to noise ratio, as has recently been found using truncations of the NRR and heterologous cleavage domains in the context of the SNIPR

synNotch receptor (Zhu et al. 2022). As the screen is both effective and scalable, it should make it possible to identify new kinds of proteolytic switches, such as the LIN-12 NRR, to optimize and diversify the current repertoire of synNotch signaling systems. Finally, the use of a model organism to test synNotch components *in vivo*, may help close the gap between the development of synNotch signaling systems and their clinical application (Brooks and Alper 2021).

Acknowledgements

Thanks to Dominic Huntley, Olivia Mosley, Abby Bryant, Navya Pampatwar, and Corey Andrews for technical assistance. Research reported in this publication was supported by the National Institutes of Health through the Institute of General Medicine of the under award number R35 GM127141 (to G.S) and the Institute of Child Health and Human Development under award number R21 HD107414 (to P.L.), in addition to support from the Roy and Diana Vagelos Precision Medicine Award (G.S., P.L.) and the Research Scholarship & Creativity Activity Program at Augusta University (to P.L.). The content is solely the responsibility of the authors and does not necessarily represent the official views of the National Institutes of Health.

Methods

Further information and requests for resources and reagents should be directed to and will be fulfilled by the Lead Contact, Paul Langridge (plangridge@augusta.edu).

Drosophila

All flies were maintained at 25°C on standard corn food. Fly stocks were maintained at 18°C, whilst experiments were performed at 25°C.

Drosophila Transgenes

All ligand and receptor coding sequences, with the exception of FSHα, were inserted into

a modified form of *pUAST-attB* (www.flyc31.org) that contains a single Flp Recombinase Target (FRT, '>') positioned between the UAS promoter and the coding sequence, and the resulting *UAS>ligand* and *UAS>receptor* transgenes were introduced at a single genomic docking site, *attP-86Fb* located on the right arm of the third chromosome, oriented so that the promoter is centromere proximal to the coding sequence. A "no promoter" (Ø) element encoding the transcriptional terminating 3' UTR of the *hsp70* gene is used in place of the UAS promoter in *Ø>ligand* transgenes (generated by Flp/FRT mitotic recombination in the male germline (Langridge and Struhl 2017)). A single *UAS.FSHα,* transgene inserted by conventional P-element mediated transformation onto the X chromosome was used in all experiments.

The WT, KtoR, and ΔIC chimeric forms of Dl (Fig. 1) are described in detail in (Langridge and Struhl 2017). Briefly, the native extracellular domain of Dl was replaced in its entirety by the β subunit of human Follicle Stimulation Hormone (FSHβ) (Fan and Hendrickson 2005) and an HRP tag was inserted immediately downstream of the C-terminal YCSFGEMKE sequence of FSHβ and immediately upstream of the Dl transmembrane domain. FSHα was co-expressed with the FSHβ-Dl protein to reconstitute FSH, which is an FSHα/FSHβ heterodimer (for simplicity, we refer to all ligands as FSH-Dl chimeras and do not include the HRP tag in their designations).

The chimeric forms of Notch (Fig. 1) are based on the FSHR-Notch receptor described in detail (Langridge and Struhl 2017). Briefly the amino-terminal Epidermal Growth Factor (EGF) Repeat containing portion of the native extracellular domain of Notch was replaced by the ectodomain of FSHR. The extracellular domain was tagged by the insertion of Cherry just upstream of the juxtamembrane NRR domain.

For the screen, the native NRR was replaced with the coding sequence of the candidate domain of interest. In each case, the same restriction enzyme sites and junction sequences were used. The sequence of the NRR insertion position is between the upstream Cherry epitope tag and the downstream Notch TM domain are as follows: delyk. . .rppanvkyvit. The amino acid

sequence of each of the ligand dependent and constitutive force sensors is given in Table S1. The *UAS KuzHA* transgene and the *UAS KuzRNAi* originate from (Coleman et al. 2010). Complete DNA sequences for both the ligands and receptors are available on request.

Analysis of signaling between dedicated ligand and receptor expressing cells.

Signaling between dedicated ligand and receptor cells was analyzed using Mosaic Analysis by Promoter Swap (MAPS; see (Langridge and Struhl 2017) for detailed description). In essence, mitotic recombination across the FRTs in cells trans-heterozygous for *UAS*> and Ø> transgenes is induced in the presence of a *nub.Gal4* driver that acts in the developing wing. Upon the appropriate segregation of the recombined chromatid arms at the 4-strand stage, this generates mutually exclusive populations of ligand and receptor expressing cells; the ligand expressing cells are marked by staining for the HRP epitope tag (blue in all the Figures), and the receptor expressing cells are marked "black" by the absence ligand expression (and when needed, red, by the Cherry epitope tag on the receptor). Signaling is monitored by assaying for ectopic expression of Cut protein from the Notch target gene *cut* in receptor expressing cells that abut ligand expressing cells along the MAPS ligand/receptor mosaic interface.

To induce mosaics by promoter swap, first or second instar larvae of the appropriate genotype (*hsp70.flp UAS.FSHα/hsp70.flp* or *Y*; *nub.Gal4/+; Ø*>*ligand/UAS*>receptor or *UAS*>*ligand/Ø*>*receptor*) were heat shocked at 36°C for one hour and wing discs from mature third instar larvae were dissected, fixed, stained for Cut and HRP expression and mounted for confocal microscopy [commercially available Mouse monoclonal anti-Cut (Mab Developmental Studies Hybridoma bank 2B10, 1/100), and Rabbit anti-HRP (Abcam ab34885, 1/1000) antisera were used in combination with Alexa 488 and 633 conjugated labelled secondary antisera following standard protocols, e.g., as in (Langridge and Struhl 2017)]. The Cherry epitope tag was also readily visualized in these preparations, although only shown in Fig. 5 and 6 (both the

HA and HRP epitopes require rabbit monoclonal antisera for detection, precluding our use of the anti-HRP antisera to mark the “ligand” clones in this context). In general, the intensity of the Cherry signal was similar for all forms of the receptors analyzed and any variation did correlate with potency of receptor activation. Expression levels of the receptor were not further considered since we compared only relative levels of cleavage of the same receptor presented with different ligands. It is also possible that receptors scored refractory to cleavage were not strongly expressed, although that was not the case for those examined in more detail, including FSHR-Notch with the native NRR excised.

Quantification and Statistical Analysis

In all *Drosophila* MAPS experiments, most if not all the imaginal wing discs contained several mutually exclusive subpopulations of ligand and receptor expressing cells within each wing primordium. In all cases, the results of each ligand/receptor combination are presented by representative images as well as quantitative analysis. As noted in the main text, Cut expression is normally induced in “border” cells flanking the D/V compartment boundary in response to native DSL/Notch signaling which peaks in the vicinity of the boundary and declines in a graded fashion as a function of distance from the boundary (Blair 1997). Signaling between FSH-Dl and FSHR-Notch chimeras along MAPS mosaic borders located away from the D/V boundary induces Cut when the combined inputs of the native and chimeric ligand/receptor interactions reach the levels normally required to induce Cut in D/V border cells. Accordingly, the distances over which MAPS mosaic borders can induce Cut away from the boundary provide an indication of the strength of the signaling interaction between the chimeric ligand and receptor.

As depicted in Figure 3A, we measured and averaged the maximum distances from the D/V boundary over which ectopic Cut was detected along 1-3 MAPS mosaic borders in each of at least 4 and typically many more discs for each genotype (power analysis>0.95, the numbers

of discs analyzed for each ligand/receptor pair are presented in Fig. 3 and 4). As disc size varies at least in part because of extra growth induced by ectopic Notch activation, we normalized the average of the distances obtained in each disc by dividing it by the width of the D/V compartment boundary within the prospective wing (the “Cut distance/DV width ratio”; Fig. 3A, y-axis).

Quantitation of the resulting ratios for each ligand/receptor pair are presented in Figures 3 and 4 in the form of boxplots in which each point depicts the average of the ratios measured for a single disc, and the mean, median, and 25-75% interquartile ranges of the ratios are depicted by a red triangle, a wide horizontal line, and the tops and bottoms of each box, respectively. Statistical comparisons of the results obtained for different ligand/receptor pairs were performed by Brown and Forsythe tests followed by Dunnett TW post-hoc analysis using *ggstatsplot* software (https://www.rstudio.com/).

Colabfold Structural Predictions

For the AlphaFold computational analysis of protein structures (Jumper and Hassabis 2022), the open-source software ColabFold (Nussinov et al. 2022) was employed (versions 1.3.0 and 1.5.2). The notebook “ColabFold: AlphaFold2 using MMseqs2” was used through the Google Collaboratory platform to run AlphaFold with the following parameters: use_templates = false, use_amber = true, msa_mode = “MMseqs2 (UniRef + Environmental)”, model_type = “AlphaFold2-ptm”, num_models = 5, model_order = [1, 2, 3, 4, 5], num_recycles = 6, rank_by = “plddt,” max_msa = null, pair_mode = “unpaired + paired”.

The amino acid sequences of the ligand-dependent domains of interest were entered to ColabFold for structure prediction using the specified parameters. No templates were used in the predictions. The AlphaFold algorithm generates five different structural models for each individual input. The models are ranked from best to worst based on the overall predicted Local Distance Difference Test (pLDDT), AlphaFold’s per-residue confidence metric. Along with the

structural models, the Predicted Aligned Error (PAE) of each model is visualized on a matrix. This metric implies a measure of confidence in the relative positions of residue pairs. The best confidence model prediction was chosen in each case and displayed in Figure S1.

Figures and Legends

Figure 1: *In vivo* screen to identify force-sensitive proteolytic switch domains

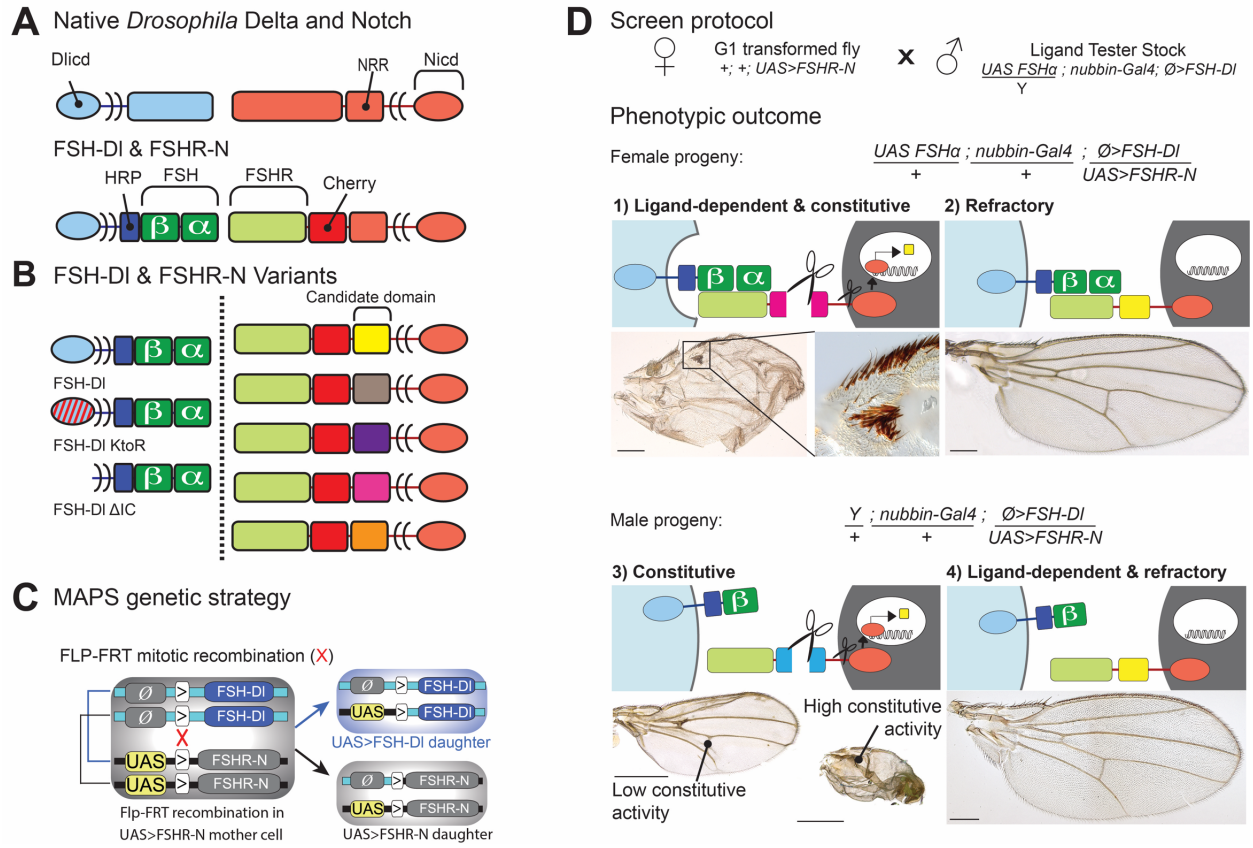

Figure 1. Functional screen to identify force-sensitive cleavage domains *in vivo*.

A. Cartoons of *Drosophila* Delta (Dl)/Notch (N) and FSH-Dl/FSHR-Notch chimeras in which the ligand binding regions of Delta/N were replaced with functional heterologous binding regions. The Dl extracellular domain was replaced by the β-subunit of Follicle Stimulating Hormone (FSHβ) and coexpression of FSHα reconstitutes the composite FSH ligand (FSH). Reciprocally, the ligand-binding (EGF) portion of the N ectodomain was replaced by the FSH receptor ectodomain (FSHR).

B. The canonical FSHR-Notch receptor was modified by replacing the NRR with a single candidate sequence to produce 43 different FSHR-Notch receptors each with distinct juxtamembrane regions. For the screen FSH-Dl was used, but for later analyses FSH-Dl was modified by replacing the Delta intracellular domain (ICD) that targets FSH-Dl into the Epsin route with ICDs that exclude the ligand from that route, either through mutation of the lysines to arginine (FSH-Dl-KtoR) or removal of the intracellular domain entirely (FSH-Dl-ΔIC).

The coding sequence for each receptor was placed downstream of a UAS promoter followed by an FRT (>) recombination target sequence to form the *UAS>FSHR-Notch* transgenes, each of which was part of a vector with one or two of several eye (w+, Rap rough eye phenotype), wing (y+), bristle (y+) or cuticle color (y+) marker genes. Mixtures of *UAS>FSHR-Notch* transgenes with distinct markers were introduced at identical genomic docking sites (86Fb) by a single micro-injection. The FSH-Dl coding sequence was placed downstream of an FRT, but no promoter (Ø), to form *Ø>FSHβ-Dl*, and inserted at the 86Fb genomic docking site.

C. To form FSH-Dl to FSHR-Notch signaling interfaces across which receptor activation can be assessed, Mosaic Analysis by Promoter Swap (MAPS) was used to induce mitotic recombination (red cross) in transheterozygous *UAS>FSHR-Notch/Ø>FSH-Dl* "mother" cells at an early stage of development. This recombination swaps the promoters to produce daughter cells that express only FSH-Dl adjacent to sibling and parental cells that express only FSHR-Notch. Only one of the two possible segregation outcomes is shown (left brackets); the alternative segregation event also results in an FSH-Dl expressing daughter cell adjacent to sibling and parental cells that express only FSHR-Notch.

D. Genotypes and possible phenotypes of screen outcross progeny. G1 female flies were crossed with male flies from a ligand tester stock with the components for both UAS/Gal4 expression in the wing and the FSH-Dl ligand: *UAS FSHα* on the X chromosome, the nubbin-Gal4 driver on the second chromosome, and the *Ø>FSHβ-Dl* transgene. FSH-Dl/FSHR-Notch interfaces were induced by MAPS (see C) and receptor

activation categorized by examining adult wing phenotypes resulting from the ectopic activation of Notch target genes: 1) Ligand-dependent and constitutive FSHR-Notch activation in the female progeny leads to ectopic wing margin and smaller wings. 2) An FSHR-Notch receptor that is refractory to cleavage when confronted with ligand produces wildtype wings in the female offspring. 3) Male progeny do not inherit the X chromosome carrying the *UAS FSHα* trangene and do not express functional FSH-Dl. If the FSHR-Notch receptor is constitutively active, receptor activation can occur even in the absence of the *UAS FSHα* trangene and male flies in this case have an abnormal wing phenotype, although to different degrees according to the extent of activation. Examples of adult wings with low and high activity levels are shown, with the major phenotype being a reduction in size, change in wing shape and ectopic wing margin. 4) In the absence of the *UAS FSHα* trangene, FSHR-Notch receptors that are ligand-dependent are not activated, resulting in a wildtype wing. Receptors refractory to cleavage will also produce wildtype wings. Scale bar 200 µm.

Figure 2: Three categories of receptor activation in the third instar imaginal wing disc

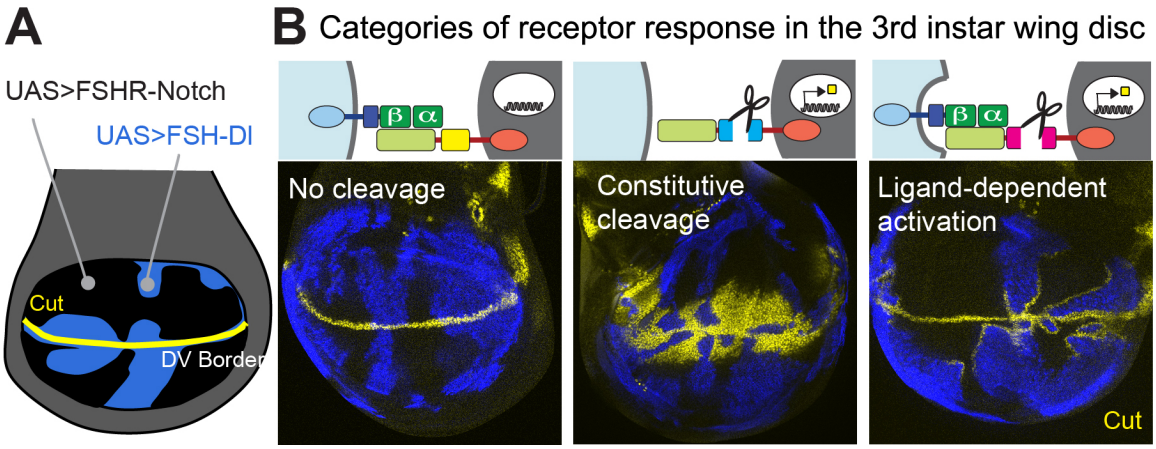

Figure 2. Three categories of receptor activation in the third instar imaginal wing disc.

A. MAPS generates mutually exclusive FSH-Dl/FSHR-Notch cell populations in the wing imaginal disc. The prospective wing (blue/black) is divided into cells expressing either FSH-Dl (the HRP epitope tag of FSH-Dl is stained blue) or receptor under Gal4/UAS control. Normally, peak levels of native DSL/N signaling induce expression of the N

target gene *cut* along the boundary between the dorsal (D) and ventral (V) compartments (Cut protein, yellow).

B. Patterns of receptor activation in the wing were divided into one of three main categories. Left, no cleavage of the candidate domain. Clones of FSH-Dl do not produce ectopic Cut at the interface with FSHR-Notch cells. Native Cut remains at the D/V boundary. Center, constitutive cleavage allows FSHR-Notch activation regardless of the presence of ligand, resulting in ectopic Cut produced in all FSHR-Notch cells whether they are close to FSH-Dl cells or not. Right, ligand-dependent activation induces cleavage of FSHR-Notch and ectopic Cut is produced only in FSHR-Notch cells adjacent to FSH-Dl cells.

Table 1 List of cleaved candidate domains

A Candidate domains cleaved in response to ligand

Name	Domain Source	Species	Size (#AA)	Description	Reason for inclusion in screen
Dscam1	Down Syndrome Cell Adhesion Molecule 1	*Drosophila*	220	Neuronal guidance receptor	Evidence that ICD acts as a transcription factor
DCC	Deleted in Colorectal Cancer/ Frazzled	*Drosophila*	18	Neuronal guidance receptor	Evidence that ICD acts as a transcription factor
EphB2	Ephrin-type receptor B2	Mouse	110	Neuronal guidance receptor	Native receptor is cleaved in response to ligand binding
DEph	Ephrin-type receptor	*Drosophila*	250	Neuronal guidance receptor	Native receptor is cleaved in response to ligand binding
Venus GFP	Venus GFP	*Aequorea victoria*	242	Entire coding region of Venus GFP	Serendipitous result
Serrate	Serrate	*Drosophila*	264	Notch ligand	Cleaved by Kuz
FAT1	FAT1	Human	93	Atypical cadherin	SNAPS: Cleavage in response to ligand
DAG	Dystroglycan	Human	261	Cell adhesion and ECM binding protein	SNAPS: Cleavage in response to ligand
NRR^{SLNR}	Notch variant	*Drosophila*	62	Variant of the NRR of Notch	LNRs removed, but S2 site remains
ephrinB	Ephrin B1 precursor ligand	Human	74	Neuronal guidance protein	Native ligand is cleaved in response to ligand binding
Flagelliform	Flagelliform F40	Spider	44	Spider silk – 40 PGGAG repeats	Biophysically demonstrated to stretch at pN forces

B Candidate domains cleaved constitutively

Name	Domain Source	Species	Size (#AA)	Description	Reason for inclusion in screen
Dephrin	Ephrin B ligand	*Drosophila*	211	Neuronal guidance protein	Native ligand is cleaved in response to ligand binding
Robo	Roundabout 1	*Drosophila*	371	Neuronal guidance receptor	DCC/Frazzled related protein
Nrg1	Neuregulin (Nrg1 type III)	Human	101	Neuronal guidance protein	ADAM10 substrate
Neogenin	Neogenin	Mouse	367	Neuronal guidance receptor	ADAM10 substrate
Eprhin B2L	Ephrin B2	Mouse	342	Neuronal guidance protein, juxtamembrane region and 2 fibronectin domains	Cleavage in response to receptor binding
Ephrin B2S	Ephrin B2	Mouse	110	Neuronal guidance protein, juxtamembrane region	Cleavage in response to receptor binding
EphB1	Ephrin B1 receptor	Human	124	Neuronal guidance receptor	Receptor cleavage in response to ligand binding
Delta	Delta	*Drosophila*	34	Notch ligand	Cleaved by Kuz
APP	Amyloid-beta precursor protein	Human	240	Neuronal repair	ADAM10 substrate
CD16	CD16	Human	194	Immune cell receptor	ADAM10 substrate
CD44	CD44	Mouse	461	Cell adhesion glycoprotein	ADAM10 substrate
Cdhr2	Cadherin-related family member 2	Human	356	Cell adhesion protein	SNAPS: Cleavage in response to ligand

Table 1. List of domains in the ligand-dependent and constitutive categories. Columns describe the domain's abbreviated name, the identity of the native source protein and species, the size of the domain (#AA=number of amino acids), a brief description of the native source protein and the reason for its inclusion in the screen.

A. Table of candidate domains cleaved in response to ligand (green), including domains classed as 'hypersensitive' (chartreuse), i.e. intermediate in response between ligand dependent and constitutive. Note that FAT1 and DAG were identified as cleaved in

response to ligand as part of the cell culture based SNAPs assay (Hayward, Aird, and Gordon 2019).

B. Table of candidate domains cleaved constitutively. Cdhr2 is cleaved constitutively, although it is reported as ligand-dependent in the SNAPs assay (Hayward, Aird, and Gordon 2019).

Domains that were not cleaved include FSHR-Notch lacking the NRR, EprinA2, *Drosophila* Fat, Filamin, Neuregulin, Starry Night, Dachsous, junctional adhesion molecule A, prion related protein, human DSCAM, viral spike proteins, epithelial cellular adhesion molecule, KIAA0319, and Muc13. The last three domains were found not to be cleaved in the SNAPs assay (Hayward, Aird, and Gordon 2019).

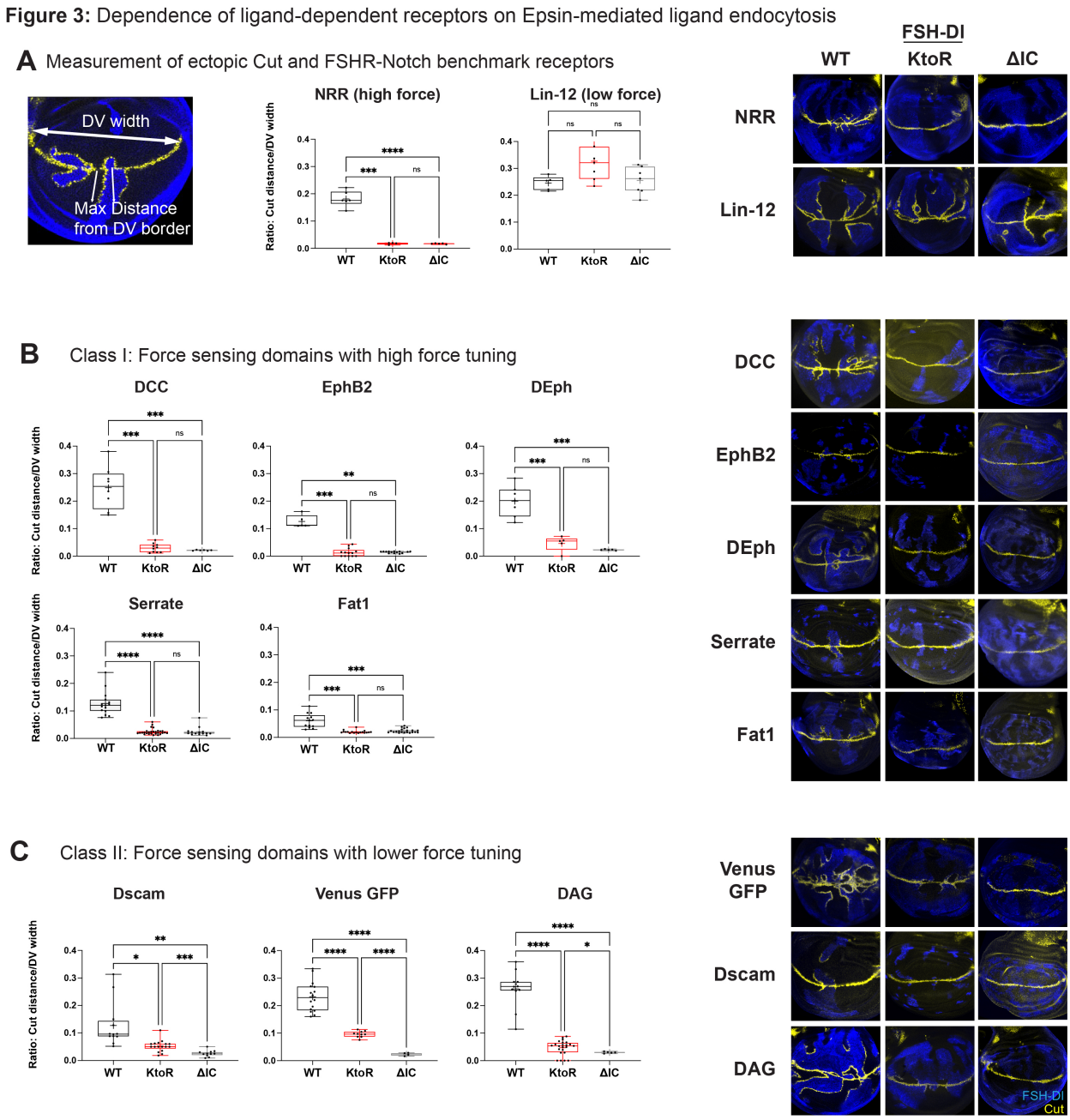

Figure 3. Dependence of ligand-dependent receptors on Epsin-mediated ligand endocytosis.

A. Quantitation of signaling between FSH-DI and FSHR-Notch receptors carrying domains cleaved in response to ligand. This was measured as the distance ectopic Cut extends away from the DV boundary relative to disc size (width of Cut expression at

the DV boundary) and presented as a ratio of the two distances (left). Signal strength is depicted as boxplots (right) that show the “cut distance/DV width” ratio for each disc as a point, as well as the mean (cross), median (horizontal line), and 25%-75% interquartile ranges (tops and bottoms of the box) for each receptor/ligand combination. Statistical comparisons of the average Cut distance/DV width ratios for each ligand/receptor pair were performed by Brown and Forsythe tests followed by Dunnett TW post-hoc analysis (see methods); *$p<0.05$, **$p<0.01$, ***$p<0.001$, and ****$p<0.0001$. Each receptor was confronted with three different FSH-Dl variants (Fig. 1A) with intracellular domains corresponding to the wildtype Dl domain (WT), the KtoR mutated Dl domain (KtoR) and a deletion of the intracellular domain (ΔIC). Representative images of these responses are shown on the far right.

As benchmarks, the response to these ligands of the canonical FSHR-Notch receptor with the *Drosophila* NRR (NRR) and FSHR-Notch with the LIN-12 NRR (LIN-12) is shown. The NRR receptor is strictly Epsin-dependent and does not show a significant response to versions of FSH-Dl that are excluded from the Epsin-route, indicating a high force tuning. In contrast, LIN-12 responds strongly to all three FSH-Dl ligands, indicating a lower force tuning.

B. Receptors with a high dependence on Epsin-mediated ligand endocytosis (Class I) have no response to ligand excluded from the Epsin route, similar to the response of the canonical FSHR-Notch with the *Drosophila* NRR.

C. Receptors with a lower dependence on Epsin-mediated ligand endocytosis (Class II) have small but detectable responses to ligand excluded from the Epsin route.

Figure 4: Class III: Hypersensitive FSHR-N receptors are cleaved constitutively and activation is enhanced by FSH-Dl on neighboring cells.

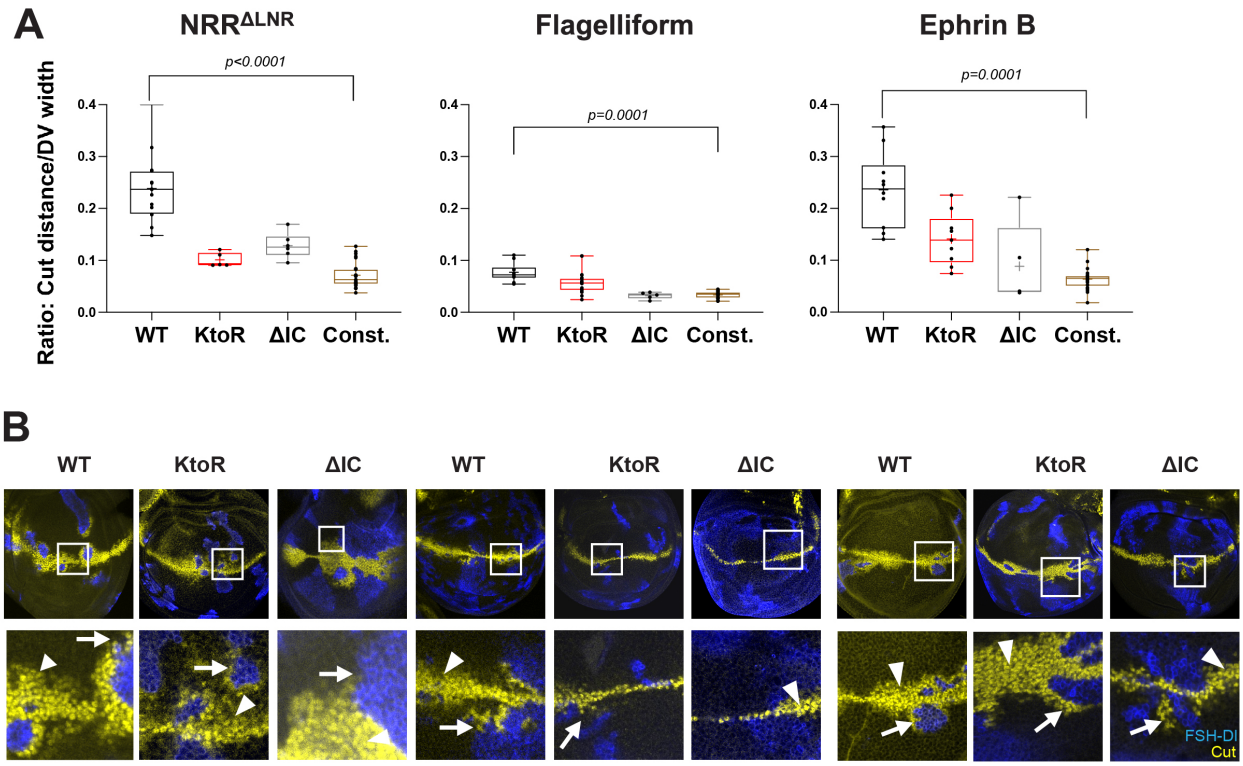

Figure 4. Hypersensitive FSHR-Notch receptors are cleaved constitutively, and activation is enhanced by FSH-Dl on neighboring cells.

A. Quantitation of signaling between FSH-Dl and FSHR-Notch 'hypersensitive' variants as in Fig. 3A. Each receptor was confronted with three different FSH-Dl variants (Fig. 1A) with intracellular domains corresponding to the wildtype Dl domain (WT), the KtoR mutated Dl domain (KtoR) and a deletion of the intracellular domain (ΔIC). In addition, the level of constitutive activation of each receptor (Const.) was measured as the maximum distance of ectopic Cut from the DV boundary in regions of the wing away from clonal interfaces.

B. Representative images showing Cut expression in MAPS mosaic wing discs for hypersensitive FSHR-Notch receptors paired with FSH-Dl, FSH-Dl KtoR or FSH-Dl ΔIC. Significant ectopic Cut is detectable in cells away from FSH-Dl cells (arrowhead, right image), but in most cases extends furthest from the DV boundary where the receptor cells meet ligand cells (arrow), quantified in A.

Figure 5: The ADAM protease Kuzbanian is required for the cleavage of candidate force sensors.

A MAPS strategy for knocking down Kuz activity in FSHR-N cells that abut FSH-DI cells.

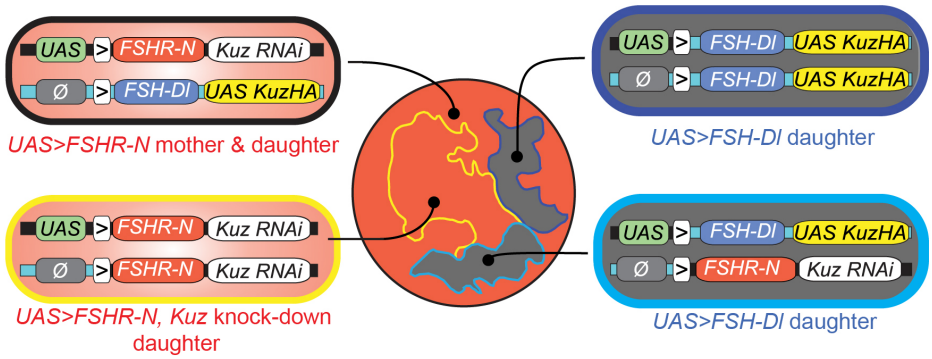

B Kuz knock-down eliminates Cut expression in FSHR-N cells that abut FSH-DI cells

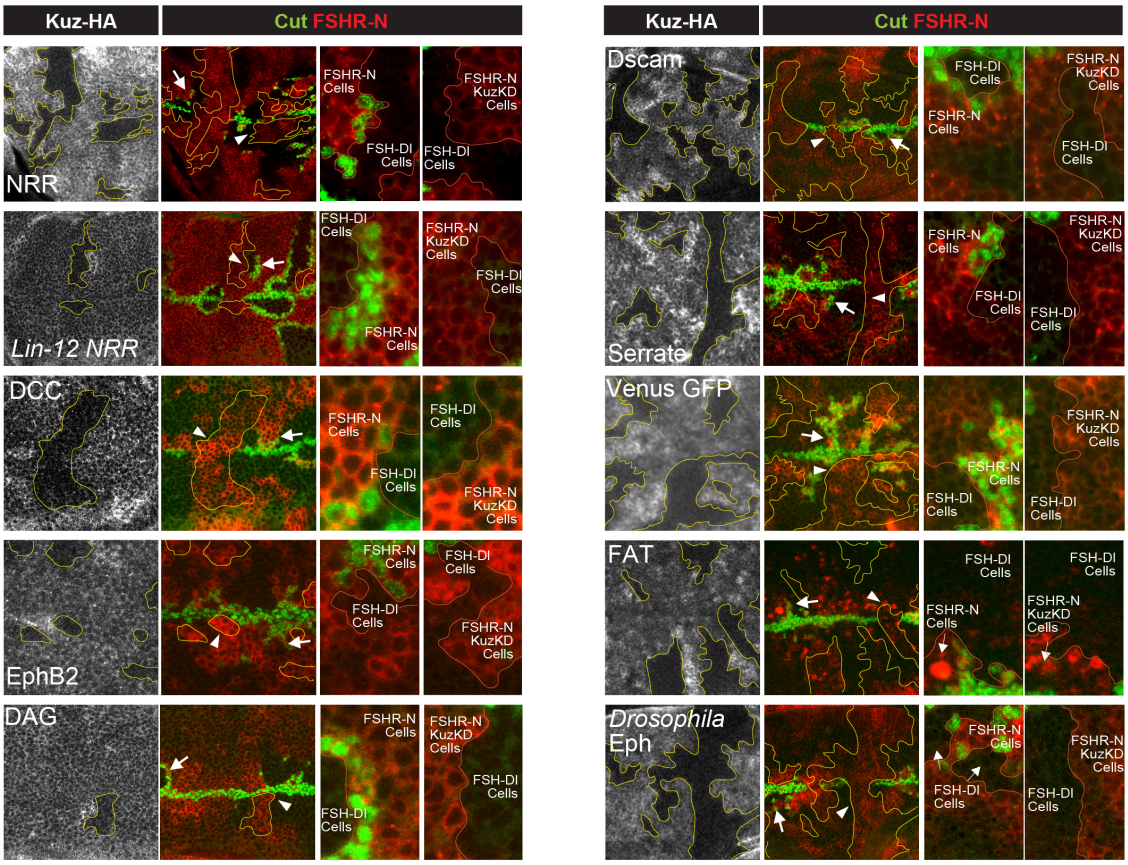

Figure 5. Kuzbanian is required for the cleavage of candidate proteolytic switch domains in response to Epsin-mediated ligand endocytosis.

A. MAPS technology used to knock-down Kuz activity in genetically marked clones of FSHR-Notch expressing cells. The expression of *UAS.Kuz-RNAi* (Kuz-RNAi) in the wing

disc reduces native Notch activation sufficiently to abolish endogenous Cut at the DV boundary, whilst co-expression of *UAS.KuzHA* rescues native DSL/Notch signaling. In background, transheterozygous "mother" cells (upper left), one chromosome carries *UAS>FSHR-Notch* with *UAS.Kuz-RNAi* positioned distally and the other chromosome carries *Ø>FSHβ-Dl* with *UAS.KuzHA* positioned distally (upper left). Cells of this "background" genotype express FSHR-Notch but not FSH-Dl and retain KuzHA function. Mitotic recombination across the FRTs generates four kinds of daughter cells, depending on the two possible segregation events (Fig S2). Two of the four, outlined in blue, are "signal-sending" cells that express FSH-Dl but not FSHR-Notch and retain Kuz function. The remaining two are "signal-receiving" cells that express FSHR-Notch but not FSH-Dl, one of which is genetically identical to the mother cell and hence retains KuzHA function (outlined in black), whereas the other is homozygous for *UAS.Kuz-RNAi* and hence subject to Kuz RNAi knock-down (outlined in yellow).
B. Comparison of the signal-receiving cells (marked by Cherry, red) in which Kuz activity is either retained (marked by HA, white) or knocked-down (marked "black" by the absence of HA) indicates that for each of the FSHR-Notch receptors shown, only clones that retain Kuz activity can express Cut (green) in response to abutting FSH-Dl signal-sending cells (marked "black" by the absence of Cherry). Arrows indicate the Cut response in Kuz positive receiving cells and arrowheads indicate the lack of response in neighboring Kuz knock-down receiving cells (shown at higher magnification to the right, with the mosaic border indicated in red). Note that where Kuz knock-down cells cross the D/V boundary they abolish the normal Cut response as expected. The identities of the candidate proteolytic domains are indicated in white font.

Figure 6: FSHR-Notch receptors with hypersensitive and constitutive activation require Kuz

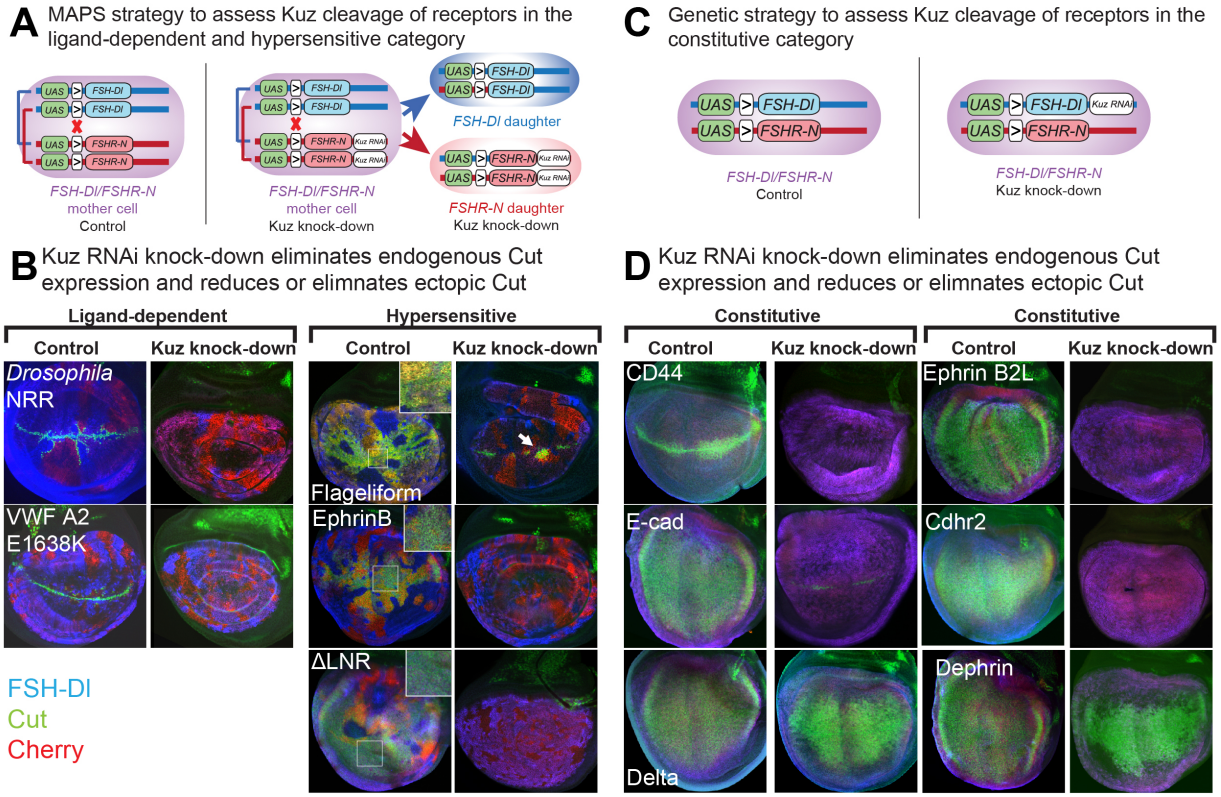

Figure 6. Kuzbanian is required for the cleavage of constitutively active FSHR-Notch receptors

A. Mitotic recombination using MAPS to compare the consequences of knocking down Kuz activity in cells that express ligand-dependent versus hyper-sensitive FSHR-Notch receptors. Left: Control genetic scheme using the 'twin spot' MAPS paradigm, with a *UAS>FSHR-Notch/UAS>FSH-Dl* parental cell and twin spot daughter cells homozygous for either *UAS>FSHR-Notch* or *UAS>FSH-Dl*. Note that in transheterozygous (mother) cells, canonical FSH-Dl and FSHR-Notch proteins mutually "cis-inactivate" each other. As a consequence, Cut activation is only induced at mosaic interfaces in which one or both clonal cell populations are homozygous for either *UAS>FSHR-Notch* or *UAS>FSH-Dl*. Right: Experimental genetic scheme to generate FSH-Dl/FSHR-Notch interfaces in which Kuz is knocked down in all FSHR-Notch expressing cells. This genotype is identical to the control scheme, except for the addition of *UAS.Kuz-RNAi* distal to *UAS>FSHR-Notch*.

B. For ligand-dependent benchmark receptors (carrying the native Notch NRR or the $A2^{E1638K}$ switch domains) in control discs in which Kuz is uniformly active (left most column), ectopic Cut is produced at mosaic borders at which one or both clonal cell populations are homozygous for either *UAS>FSHR-Notch* or *UAS>FSH-Dl* (first column). In the Kuz knock-down discs (second column), native DSL/Notch signaling is sufficiently impaired that Cut is not induced along the D/V boundary, and FSH-Dl/FSHR-Notch signaling also fails to induce Cut for the Notch NRR or $A2^{E1638K}$ receptors. For the hypersensitive receptors carrying the Flageliform, EphrinB and ΔLNR candidate domains, control wing discs show extensive Cut activation in most FSHR-Notch cells (insets), but not in homozygous *UAS>FSH-Dl* clonal populations, which lack the *UAS>FSHR-Notch* transgene (third column). We infer that this Cut activation reflects constitutive activity of the receptor. In contrast, the experimental Kuz knock-down discs do not express Cut, except in homozygous *UAS>FSHR-Notch* clones encoding the

Flageliform receptor positioned close to the D/V border (arrow), which we interpret as due to residual Kuz activity.

C. Genotypes for testing if Kuz is required for the transducing activity of constitutively active FSHR-Notch receptors. Both control (wild type for *Kuz*) and experimental (Kuz knock-down) animals are *UAS>FSHR-Notch/UAS>FSH-Dl*, with experimental animals also carrying *UAS.Kuz-RNAi* in *cis* with *UAS>FSH-Dl*.

D. Cut is uniformly expressed throughout most or all of the wing pouch of control animals, except in the case of the CD44 receptor, where it is ectopically expressed only in the vicinity of the D/V border (from which we infer that it has weak constitutive activity, sufficient only to boost the higher levels of native DSL/Notch signaling in the vicinity of the border to generate an ectopic Cut response). The Cut response is abolished for the CD44, E-cad, Ephrin B2L and Cdhr2 receptors, but not the Delta and Dephrin receptors.

Figure S1 Structural predictions of each of the candidate domains cleaved in response to ligand

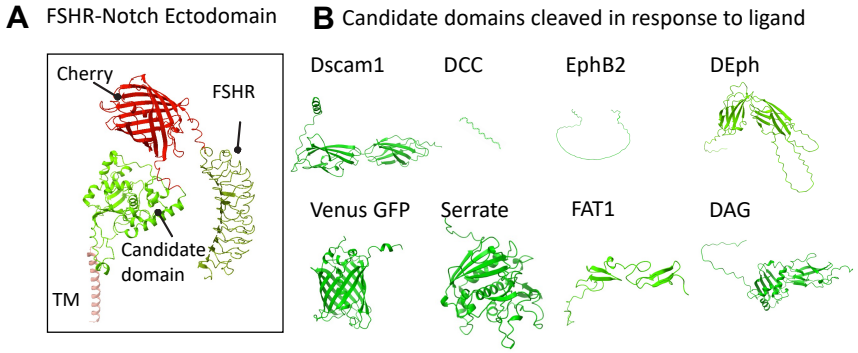

Figure S1. Structural predictions of each of the candidate domains cleaved in response to ligand.

A. High confidence structural predictions of domains showing ligand-dependent cleavage. The 3D structure of the entire extracellular region of canonical FSHR-Notch

was predicted using AlphaFold [(Jumper and Hassabis 2022) see materials and methods].

B. This prediction was repeated for receptors with each of the candidate domains, and in each image only the candidate domain is shown and the remaining receptor hidden. Each candidate has a distinct structure with few commonalities. PDB files for each case are available.

Figure S2 Genetic scheme for producing Kuz RNAi knock-down using MAPS.

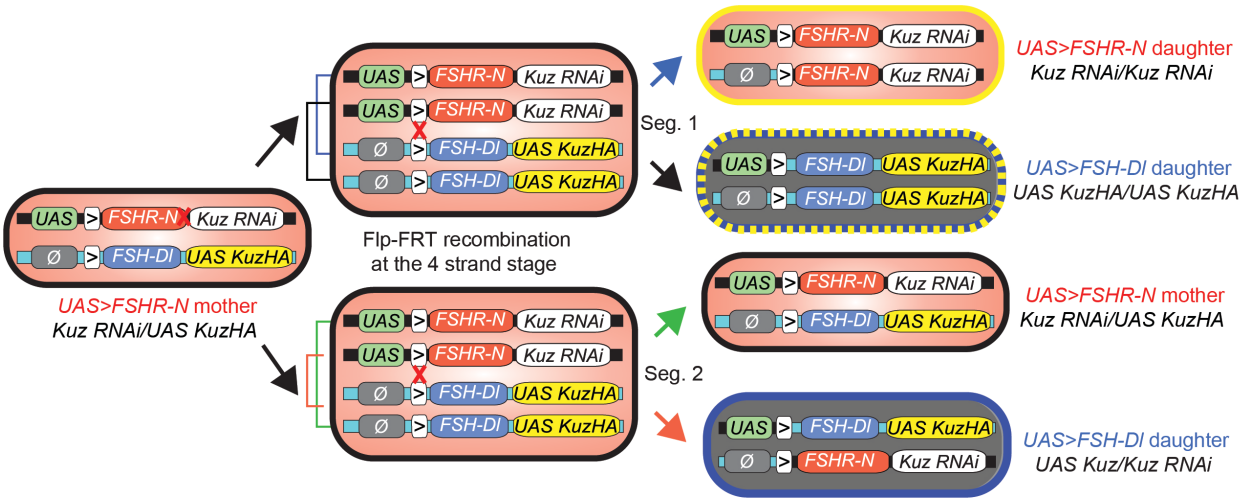

Figure S2. Genetic scheme for producing Kuz RNAi knock-down using MAPS.

Mitotic recombination using MAPS to remove detectable Kuz activity in sub-populations of FSHR-Notch cells. *UAS Kuz RNAi* was positioned distal to the *UAS>FSHR-Notch* transgene and *UAS KuzHA* distal to the *Ø>FSHβ-Dl* transgene. MAPS mitotic recombination at the four strand stage results in four possible segregant daughter cells (right and Fig 5A), including one with the genotype identical to the mother cell.

Table S1 **A)** Amino acid sequences of domains that are cleaved in response to ligand.

Name	Domain Source	Species	Amino Acid Sequence
Dscam1	Down Syndrome Cell Adhesion Molecule 1	*Drosophila*	VLAPPQSPHVTLSATTTDALTVKLKPHEGDTAPLHGYTLHYKPEFGEWETSEVSVDSQKHNIEGLLCGSRYQVYATGFNNIGAGEASDI LNTRTKGQKPKLPEKPRFIEVSSNSVSLHFKAWKDGGCPMSHFVVESKKRDQIEWNQISNNVKPDNNYVVLDLEPATWYNLRITAH NSAGFTVAEYDFATLTVTGGTIAPSRDLPELSAEDTIRIILSNLN
DCC	Deleted in Colorectal Cancer/ Frazzled	*Drosophila*	VTMQEPDTIAKGIDNEKL
EphB2	Ephrin-type receptor B2	Mouse	APSAVSIMHQVSRTVDSITLSWSQPDQPNGVILDYELQYYEKQELSEYNATAIKSPTNTVTVQGLKAGAIYVFQVRARTVAGYGRYSG KMYFQTMTEAEYQTSIKEKLP
DEph	Ephrin-type receptor	*Drosophila*	APTNLTLLFVDQTSAIISWSAPAKNESFSSETNSKIYHSDIVYKIKCNICSPNVVYNP STDTFNETKITLTNLEPVTTYTVQIHAINSVSHINEFKRHSNESSLVAVSDIVFSNTSLLNIPLDLNEVKTGQAEIVFTTESVLLSTVFNLRIL AITNKDADLEWDKPVQSDFPLEFYEVRWFPKVELDAINKSALNTKETKAHIVGLLENTEYGFQVRCKTNNGFGSYSNMIYAQTLQSV GSVYDDSVQI
Venus GFP	Venus GFP	*Aequorea victoria*	MVSKGEELFTGVVPILVELDGDVNGHKFSVSGEGEGDATYGKLTLKLICTTGKLPVPWPTLVTTLGYGLQCFARYPDHMKQHDFFKSA MPEGYVQERTIFFKDDGNYKTRAEVKFEGDTLVNRIELKGIDFKEDGNILGHKLEYNYNSHNVYITADKQKNGIKANFKIRHNIEDGGV QLADHYQQNTPIGDGPVLLPDNHYLSYQSKLSKDPNEKRDHMVLLEFVTAAGITLGMDELYK
Serrate	Serrate	*Drosophila*	DPKSACQNASNTISPYTALNRSQNWLDIALTGRTEDDENCNACVCENGTSRCTNLWCGLPNCYKVDPLSKSSNLSGVCKQHEVCVP ALSETCLSSPCNVRGDCRALEPSRRVAPPRLPAKSSCWPNQAVVNENCARLTILLALERVGKGASVEGLCSLVRVLLAAQLIKKPASTFG QDPGMLMVLCDLKTGTNDTVELTVSSSKLNDPQLPVAVGLLGELLSFRQLNGIQRRKELELQHAKLAALTSIVEVKLETARVADGSGH
FAT1	FAT1	Human	LSPYCKDEPCKNGGTCFDSLDGAVCQCDSGFRGERCQSDIDECSGNPCLHGALCENTHGSYHCNCSHEYRGRHCEDAAPNQYVSTP WNIGLAE
DAG	Dystroglycan	Human	GGEPNQRPELKNHIDRVDAWVGTYFEVKIPSDTFYDHEDTTTDKLKLTLKLREQQLVGEKSWVQFNSNSQLMYGLPDSSHVGKHEY FMHATDKGGLSAVDAFEIHVHRRPQGDRAPARFKAKFVGDPALVLNDIHKKIALVKKLAFAFGDRNCSTITLQNITRGSIVVEWTNNT LPLEPCPKEQIAGLSRRIAEDDGKPRPAFSNALEPDFKATSITVTGSGSCRHLQFIPVVPPRRVPSEAPPTEVPDRDPEKSSEDDV
NRR$^{\Delta LNR}$	Notch variant	*Drosophila*	DIYDANYPGWNGGSGSTAAKHQLRNDFQIHSVRGIKNPGDEDNGEPPANVKYVITGIILVII
ephrinB	Ephrin B1 precursor ligand	Human	DPNAVTPEQLTTSRPSKEADNTVKMATQAPGSRGSLGDSDGKHETVNQEEKSGPGASGGSSGDPDGFFNSKVAL
Flagelliform	Flagelliform F40	Spider	GPGGAGPGGAGPGGAGPGGAGPGGAGPGGAGPGGAGPGGA

B) Amino acid sequences of domains that are constitutively cleaved

Name	Domain Source	Species	Amino Acid Sequences
Dephrin	Ephrin B ligand	*Drosophila*	CAPEDNNKTTALSNSKSVTDTGGAINVNIANNDESHVNSHGNNIAIGTNIGINGGQIIGGPQSAGIPINPLSGNNNINGIPTTINSNIDQFNRIPIQPNIIG NHVGTNAVGTGIVGGGGIILTPGHAHGNINMLQPGRGGINGAYPGHHHIQTGIRINNVPTQHNYPSHKGNANSNINGNDDHHHYNKHPNEVVKNEE LTYNSGAATSDGN
Robo	Roundabout 1	*Drosophila*	PPGTPKVLNVSRTSISLRWAKSQEKPGAVGPIIGYTVEYFSPDLQTGWIVAAQRVGDTQVTISGLTPGTSYVFLVRAENTQGISVPSGLSNTIKTIEADFDAA SANDLSGARTLLTGKSVELIDASAINASAVRLEWMLHVSADEKYVEGLRIHYKDASVPSAQYHSITVMDASAESFVVGNLKKYTKYEFFLTPFFETIEGQPS NSKTALTYEDVPSAPPDNIQIGMYNQTAGWVRWTPPPSQHHNGNLYGYKIEVSAGNTMKVLANMTLNATTTSVLLNNLTTGAVYSVRLNSFTK AGDGPYSKPISLFMDPTHHVHPPRAHPSGTHDGRHEGQDLTYHNNGNIPPGDINPTTHKKTTDYLSGP
Nrg1	Neuregulin (Nrg1 type III)	Human	VESNEIITGMPASTEGAYVSSATSTSTTGTSHLVKCAEKEKTFCVNGGECFMVKDLSNPSYLCKCPNEFTGDRCQNYVMASFYKHLGIEFMEAEELYQKR
Neogenin	Neogenin	Mouse	VPSSLHVRPLVTSIVVSWTPPENQNIVVRGYAIGYGIGSPHAQTIKVDYKQRYYTIENLDPSSHYVITLKAFNNVGEGIPLYESAVTRPHTDTSEVDLFVINAP YTPVPDPTPMMPPVGVQASILSHDTIRITWADNSLPKHQKITDSRYYTVRWKTNIPANTKYKNANATTLSYLVTGLKPNTLYEFSVMVTKGRRSSTWSMT AHGATFELVPTSPPKDVTVVSKEGKPRTIIVNWQPP SEANGKITGYIIYYSTDVNAEIHDWVIEPVVGNRLTHQIQELTLDTPYYFKIQARNSKGMGPMSEAVQFRTPKADSSDKMPNDQALGSAGKGSRLPDLGS DYKPPMSGSNSPHGSPTSPLDSNML
Eprhin B2L	Ephrin B2	Mouse	MAMARSRRDSVWKYCWGLLMVLCRTAISRSIVLEPIYWNSSNSKFLPGQGLVLYPQIGDKLDIICPKVDSKTVGQYEYYKVYMVDKDQADRCTIKKENTP LLNCARPDQDVKFTIKFQEFSPNLWGLEFQKNKDYYIISTSNGSLEGLDNQEGGVCQTRAMKILMKVGQDASSAGSARNHGPTRRPELEAGTNGRSSTT SPFVKPNPGSSTDGNSAGHSGNNLLGSEVALFA
Ephrin B2S	Ephrin B2	Mouse	GQDASSAGSARNHGPTRRPELEAGTNGRSSTTSPFVKPNPGSSTDGNSAGHSGNNLLGSEVALFA
EphB1	Ephrin B1 receptor	Human	PFPPQHVSVNITTNQAAPSTVPIMHQVSATMRSITLSWPQPEQPNGIILDYEIRYYEKEHNEFNSSMARSQTNTARIDGLRPGMVYVVQVRARTVAGYG KFSGKMCFQTLTDDDYKSELREQLP
Delta	Delta	*Drosophila*	DEESYDSVTFDAHQYGATTQARADGLANAQV
APP	Amyloid-beta precursor protein	Human	MVSKGEEDNSDVWWGGADTDYADGSEDKVVEVAEEEEVAEVEEEEADDDEDDEDGDEVEEEAEEPYEEATERTTSIATTTTTTTESVEEVVRVPTTAAS TPDAVDKYLETPGDENEHAHFQKAKERLEAKHRERMSQVMREWEEAERQAKNLPKADKKAVIQHFQEKVESLEQEAANERQQLVETHMARVEAML NDRRRLALENYITALQAVPPRPRHVFNMLKKYVRAEQKDRQHTLKHFEHVRMVDPKKAAQIRSQVMTHLRVIYERMNQSLSLLYNVPAVAEEIQDEVD ELLQKEQNYSDDVLANMISEPRISYGNDALMPSLTETKTTVELLPVNGEFSLDDLQPWHSFGADSVPANTENEVEPVDARPAADRGLTTRPGSGLTNIKT EEISEVNLDAEFRHDSGYEVHHQKLVFFAEDVGSNKGR
CD16	CD16	Human	GMRTEDLPKAVVFLEPQWYRVLEKDSVTLKCQGAYSPEDNSTQWFHNESLISSQASSYFIDAATVDDSGEYRCQTNLSTLSDPVQLEVHIGWLLLQAPR WVFKEEDPIHLRCHSWKNTALHKVTYLQNGKGRKYFHHNSDFYIPKATLKDSGSYFCRGLFGSKNVSSETVNITITQGLAVSTISSFFPPGYQV

B) Amino acid sequences of domains that are constitutively cleaved

Name	Domain Source	Species	Amino Acid Sequences
CD44	CD44	Mouse	HSKSHAAAQKQNNWIWSWFGNSQSTTQTQEPTTSATTALMTTPETPPKRQEAQNWFSWLFQPSESKSHLHTTTKMPGTESNTNPTGWEPNEENED ETDKYPSFSGSGIDDDEDFISSTIASTPRVSARTEDNQDWTQWKPNHSNPEVLLQTTTRMADIDRISTSAHGENWTPEPQPPFNNHEYQDEEETPHATS TTPNSTAEAAATQQETWFQNGWQGKNPPTPSEDSHVTEGTTASAHNNHPSQRITTQSQEDVSWTDFFDPISHPMGQGHQTESKDTDSSHS TTLQPTAAPNTHLVEDLNRTGPLSVTTPQSHSQNFSTLHGEPEEDENHPTTSILPSSTKS GAKDARRGGSLPTDTTTSVEGYTFQYPDTMENGTLFPVTPAKTEVFGETEVTLATDSNVNVDGSLPGDRDSSKDSRGSSRTVTHGSELAGHSSANQDSG VTTTSGPMRRPQIPER
Cdhr2	Cadherin-related family member 2	Human	VNDNPPTLDVASLRGIRVAENGSQHGQVAVVVASDVDTSAQLEIQLVNILCTKAGVDVGSLCWGWFSVAANGSVYINQSKAIDYEACDLVTLVVRACDL ATDPGFQAYSNNGSLLITIEDVNDNAPYFLPENKTFVIIPELVLPNREVASVRARDDDSGNNGVILFSILRVDFISKDGATIPFQGVFSIFTSSEADVFAGSIQP VTSLDSTLQGTYQVTVQARDRPSLGPFLEATTTLNLFTVDQSYRSRLQFSTPKEEVGANRQAINAALTQATRTTVYIVDIQDIDSAARARPHSYLDAYFVFP NGSALTLDE LSVMIRNDQDSLTQLLQLGLVVLG SQESQESDLSKQLIS

Bischof, J, R K Maeda, M Hediger, F Karch, and K Basler. 2007. 'An optimized transgenesis system for Drosophila using germ-line-specific ϕC31 integrases', *Proceedings of the National Academy of Sciences*, 104: 3312-17.

Blair, S. S. 1997. 'Limb development: marginal fringe benefits', *Curr Biol*, 7: R686-90.

Brand, A H, and N Perrimon. 1993. 'Targeted gene expression as a means of altering cell fates and generating dominant phenotypes.', *Development*, 118: 401-15.

Brooks, S. M., and H. S. Alper. 2021. 'Applications, challenges, and needs for employing synthetic biology beyond the lab', *Nature Communications*, 12: 1390.

Brou, C, F Logeat, N Gupta, C Bessia, O LeBail, J R Doedens, A Cumano, P Roux, R A Black, and A Israel. 2000. 'A novel proteolytic cleavage involved in Notch signaling: the role of the disintegrin-metalloprotease TACE.', *Molecular Cell*, 5: 207-16.

Caescu, C. I., G. R. Jeschke, and B. E. Turk. 2009. 'Active-site determinants of substrate recognition by the metalloproteinases TACE and ADAM10', *Biochemistry Journal*, 424: 79-88.

Coleman, H A, J P Labrador, R K Chance, and G J Bashaw. 2010. 'The Adam family metalloprotease Kuzbanian regulates the cleavage of the roundabout receptor to control axon repulsion at the midline', *Development*, 137: 2417-26.

Crawley, J. T., R. de Groot, Y. Xiang, B. M. Luken, and D. A. Lane. 2011. 'Unraveling the scissile bond: how ADAMTS13 recognizes and cleaves von Willebrand factor', *Blood*, 118: 3212-21.

de Celis, J F, A Garcia-Bellido, and S J Bray. 1996. 'Activation and function of Notch at the dorsal-ventral boundary of the wing imaginal disc.', *Development*, 122: 359-69.

De Strooper, B, W Annaert, P Cupers, P Saftig, K Craessaerts, J S Mumm, E H Schroeter, V Schrijvers, M S Wolfe, W J Ray, A Goate, and R Kopan. 1999. 'A presenilin-1-dependent gamma-secretase-like protease mediates release of Notch intracellular domain.', *Nature*, 398: 518-22.

Diaz-Benjumea, F J, and S M Cohen. 1995. 'Serrate signals through Notch to establish a Wingless-dependent organizer at the dorsal/ventral compartment boundary of the Drosophila wing.', *Development*, 121: 4215-25.

Doherty, D, G Feger, S Younger-Shepherd, L Y Jan, and Y N Jan. 1996. 'Delta is a ventral to dorsal signal complementary to Serrate, another Notch ligand, in Drosophila wing formation.', *Genes & Development*, 10: 421-34.

Fan, Q. R., and W. A. Hendrickson. 2005. 'Structure of human follicle-stimulating hormone in complex with its receptor', *Nature*, 433: 269-77.

Gazave, Eve, Pascal Lapébie, Gemma S Richards, Frédéric Brunet, Alexander V Ereskovsky, Bernard M Degnan, Carole Borchiellini, Michel Vervoort, and Emmanuelle Renard. 2009. 'Origin and evolution of the Notch signalling pathway: an overview from eukaryotic genomes', *BMC Evolutionary Biology*, 9: 249-27.

Golic, K G. 1991. 'Site-specific recombination between homologous chromosomes in Drosophila.', *Science*, 252: 958-61.

Gordon, W R, B Zimmerman, L He, L J Miles, and J Huang. 2015. 'Mechanical allostery: Evidence for a force requirement in the proteolytic activation of Notch', *Developmental Cell*, 33: 729-36.

Greene, Adrienne C, Samuel J Lord, Aiwei Tian, Christopher Rhodes, Hiroyuki Kai, and Jay T Groves. 2014. 'Spatial organization of EphA2 at the cell-cell interface modulates trans-endocytosis of ephrinA1.', *Biophysical Journal*, 106: 2196-205.

Greenwald, I. 1998. 'LIN-12/Notch signaling: lessons from worms and~flies', *Genes & Development*, 12: 1751-62.

Hayashida, Kazutaka, Allison H Bartlett, Ye Chen, and Pyong Woo Park. 2010. 'Molecular and Cellular Mechanisms of Ectodomain Shedding', *The Anatomical Record: Advances in Integrative Anatomy and Evolutionary Biology*, 293: 925-37.

Hayward, Amanda N, Eric J Aird, and Wendy R Gordon. 2019. 'A toolkit for studying cell surface shedding of diverse transmembrane receptors.', *eLife*, 8.

Janes, Peter W, Nayanendu Saha, William A Barton, Momchil V Kolev, Sabine H Wimmer-Kleikamp, Eva Nievergall, Carl P Blobel, Juha-Pekka Himanen, Martin Lackmann, and Dimitar B Nikolov. 2005. 'Adam Meets Eph: An ADAM Substrate Recognition Module Acts as a Molecular Switch for Ephrin Cleavage In trans', *Cell*, 123: 291-304.

Jumper, J., and D. Hassabis. 2022. 'Protein structure predictions to atomic accuracy with AlphaFold', *Nat Methods*, 19: 11-12.

Kidd, S, T Lieber, and M W Young. 1998. 'Ligand-induced cleavage and regulation of nuclear entry of Notch in Drosophila melanogaster embryos', *Genes & Development*, 12: 3728-40.

Kovall, Rhett A, Brian Gebelein, David Sprinzak, and Raphael Kopan. 2017. 'The Canonical Notch Signaling Pathway: Structural and Biochemical Insights into Shape, Sugar, and Force', *Developmental Cell*, 41: 228-41.

Langridge, Paul D, Alejandro Garcia Diaz, Jessica Yu Chan, Iva Greenwald, and Gary Struhl. 2022. 'Evolutionary plasticity in the requirement for force exerted by ligand endocytosis to activate C. elegans Notch proteins.', *Current biology : CB*, 32: 2263-71.e6.

Langridge, Paul D, and Gary Struhl. 2017. 'Epsin-dependent ligand endocytosis activates Notch by force.', *Cell*, 171: 1383-96.

Lecourtois, M., and F. Schweisguth. 1998. 'Indirect evidence for Delta-dependent intracellular processing of notch in Drosophila embryos', *Current Biology*, 8: 771-4.

Lichtenthaler, S. F., M. K. Lemberg, and R. Fluhrer. 2018. 'Proteolytic ectodomain shedding of membrane proteins in mammals-hardware, concepts, and recent developments', *EMBO Journal*, 37.

Lieber, Toby, Simon Kidd, and Michael W Young. 2002. 'Kuzbanian-mediated cleavage of Drosophila Notch.', *Genes & Development*, 16: 209-21.

Lipper, C. H., K. H. Gabriel, T. C. M. Seegar, K. L. Durr, M. G. Tomlinson, and S. C. Blacklow. 2022. 'Crystal structure of the Tspan15 LEL domain reveals a conserved ADAM10 binding site', *Structure*, 30: 206-14 e4.

Marston, Daniel J, Sarah Dickinson, and Catherine D Nobes. 2003. 'Rac-dependent trans-endocytosis of ephrinBs regulates Eph-ephrin contact repulsion.', *Nature Cell Biology*, 5: 879-88.

Morsut, Leonardo, Kole T Roybal, Xin Xiong, Russell M Gordley, Scott M Coyle, Matthew Thomson, and Wendell A Lim. 2016. 'Engineering customized cell sensing and response behaviors using synthetic Notch receptors.', *Cell*, 164: 780-91.

Neuhaus-Follini, Alexandra, and Greg J Bashaw. 2015. 'The Intracellular Domain of the Frazzled/DCC Receptor Is a Transcription Factor Required for Commissural Axon Guidance.', *Neuron*, 87: 751-63.

Nussinov, R., M. Zhang, Y. Liu, and H. Jang. 2022. 'AlphaFold, Artificial Intelligence (AI), and Allostery', *Journal Physical Chemistry B*, 126: 6372-83.

Overstreet, E, E Fitch, and J A Fischer. 2004. 'Fat facets and Liquid facets promote Delta endocytosis and Delta signaling in the signaling cells', *Development*, 131: 5355-66.

Pan, D, and G M Rubin. 1997. 'Kuzbanian controls proteolytic processing of Notch and mediates lateral inhibition during Drosophila and vertebrate neurogenesis.', *Cell*, 90: 271-80.

Roybal, Kole T, Levi J Rupp, Leonardo Morsut, Whitney J Walker, Krista A McNally, Jason S Park, and Wendell A Lim. 2016. 'Precision tumor recognition by T cells with combinatorial antigen-sensing circuits.', *Cell*, 164: 770-79.

Schroeter, E. H., J. A. Kisslinger, and R. Kopan. 1998. 'Notch-1 signalling requires ligand-induced proteolytic release of intracellular domain', *Nature*, 393: 382-6.

Seegar, Tom C M, Lauren B Killingsworth, Nayanendu Saha, Peter A Meyer, Dhabaleswar Patra, Brandon Zimmerman, Peter W Janes, Eric Rubinstein, Dimitar B Nikolov, Georgios Skiniotis, Andrew C Kruse, and Stephen C Blacklow. 2017. 'Structural Basis for Regulated Proteolysis by the α-Secretase ADAM10.', *Cell*, 171: 1638-48.e7.

Sloas, D. C., J. C. Tran, A. M. Marzilli, and J. T. Ngo. 2023. 'Tension-tuned receptors for synthetic mechanotransduction and intercellular force detection', *Nat Biotechnol*, 41: 1287-95.

Struhl, G, and A Adachi. 1998. 'Nuclear access and action of Notch in vivo.', *Cell*, 93: 649-60.

Struhl, G, and I Greenwald. 1999. 'Presenilin is required for activity and nuclear access of Notch in Drosophila.', *Nature*, 398: 522-25.

Struhl, G., and A. Adachi. 2000. 'Requirements for presenilin-dependent cleavage of notch and other transmembrane proteins', *Molecular Cell*, 6: 625-36.

Tosetti, F., M. Alessio, A. Poggi, and M. R. Zocchi. 2021. 'ADAM10 Site-Dependent Biology: Keeping Control of a Pervasive Protease', *International Journal Molecular Science*, 22.

Tsai, H M, I I Sussman, and R L Nagel. 1994. 'Shear stress enhances the proteolysis of von Willebrand factor in normal plasma.', *Blood*, 83: 2171-79.

Wang, W, and G Struhl. 2004. 'Drosophila Epsin mediates a select endocytic pathway that DSL ligands must enter to activate Notch', *Development*, 131: 5367-80.

Wang, W., and G. Struhl. 2005. 'Distinct roles for Mind bomb, Neuralized and Epsin in mediating DSL endocytosis and signaling in Drosophila', *Development*, 132: 2883-94.

Weskamp, G., J. W. Ford, J. Sturgill, S. Martin, A. J. Docherty, S. Swendeman, N. Broadway, D. Hartmann, P. Saftig, S. Umland, A. Sehara-Fujisawa, R. A. Black, A. Ludwig, J. D. Becherer, D. H. Conrad, and C. P. Blobel. 2006. 'ADAM10 is a principal 'sheddase' of the low-affinity immunoglobulin E receptor CD23', *Nat Immunol*, 7: 1293-8.

Zang, Y., K. Chaudhari, and G. J. Bashaw. 2021. 'New insights into the molecular mechanisms of axon guidance receptor regulation and signaling', *Curr Top Dev Biol*, 142: 147-96.

Zhang, Qing, Yan-Feng Zhou, Cheng-Zhong Zhang, Xiaohui Zhang, Chafen Lu, and Timothy A Springer. 2009. 'Structural specializations of A2, a force-sensing domain in the ultralarge

vascular protein von Willebrand factor.', *Proceedings of the National Academy of Sciences*, 106: 9226-31.

Zhu, I., R. Liu, J. M. Garcia, A. Hyrenius-Wittsten, D. I. Piraner, J. Alavi, D. V. Israni, B. Liu, A. S. Khalil, and K. T. Roybal. 2022. 'Modular design of synthetic receptors for programmed gene regulation in cell therapies', *Cell*, 185: 1431-43 e16.